Journal of Zhejiang University-SCIENCE B (Biomedicine & Biotechnology) *in press*
www.jzus.zju.edu.cn; www.springer.com/journal/11585
E-mail: jzus_b@zju.edu.cn

Research Article

https://doi.org/10.1631/jzus.B2500346

5-Fluorouracil causes intestinal damage via gut microbiota-mediated ferroptosis and innate immunity in *Drosophila melanogaster* and mice

Xiaoqian WANG[1], Minghui XIU[1,2], Linghui CHANG[1], Jinhan WU[2], Yan WANG[2], Jianzheng HE[1,3,4]✉, Yongqi LIU[2,3]✉

[1]*Provincial-level Key Laboratory for Molecular Medicine of Major Diseases and The Prevention and Treatment with Traditional Chinese Medicine Research in Gansu Colleges and University, Gansu University of Chinese Medicine, Lanzhou 730000, China*
[2]*College of Public Health, Gansu University of Chinese Medicine, Lanzhou 730000, China*
[3]*Key Laboratory of Dunhuang Medicine, Ministry of Education, Lanzhou 730000, China*
[4]*NHC Key Laboratory for Diagnosis and Therapy of Gastrointestinal Tumor, Gansu Provincial Hospital, Lanzhou 730000, China*

Abstract: Chemotherapy-induced intestinal mucositis (IM) severely impacts cancer prognosis, yet effective therapies remain limited due to unclear mechanisms. This study aimed to establish a 5-fluorouracil (5-FU)-induced IM model in *Drosophila melanogaster* (flies). The results revealed that 5-FU caused systemic and intestinal damage in flies, including reduced survival rate, starvation resistance, development, excretion, crop motility and intestinal length; disrupted acid-base homeostasis; and increased enterocyte death. The combined analysis of transcriptomics, bioinformatics, and microbiomics demonstrated that intestinal damage induced by 5-FU was associated with gut microbiota imbalance, ferroptosis, and innate immunity. 5-FU consistently activated ferroptosis in flies, including increased reactive oxygen species (ROS), malondialdehyde (MDA), total Fe^{2+}, lipid peroxidation, and the expression of key ferroptosis-related genes. Ferroptosis inhibitor improved survival rates and intestinal damage in 5-FU-treated flies. Furthermore, antibiotic depletion of gut microbiota alleviated intestinal damage and down-regulated innate immune and ferroptosis markers in 5-FU-induced flies. Conversely, fecal microbiota transplantation (FMT) from 5-FU-induced flies was sufficient to recapitulate intestinal injury in healthy flies. 5-FU also consistently induced intestinal damage and ferroptosis in mice, including increased ROS, ACSL4, and 4-HNE levels, and decreased GPX4. This study implicates gut microbiota-driven ferroptosis and innate immunity in 5-FU-induced IM, establishing *Drosophila melanogaster* as a powerful model for mechanistic discovery and drug screening.

Key words: Intestine mucositis; 5-Fluorouracil (5-FU); Gut microbiota; Ferroptosis; *Drosophila melanogaster*

1 Introduction

Chemotherapy is the primary clinical treatments for cancer, although it leads to a range of side effects, such as gastrointestinal damage and bone marrow suppression (Elad et al., 2020). Patients receiving high-dose chemotherapy frequently experience nausea, vomiting, diarrhea and pain, which is a sign of intestinal mucositis (IM) (Elad, et al., 2020; Di Nardo et al., 2022; Jurica and Turjap, 2025). IM is a common side effect of several chemotherapeutic agents and is characterized by mucositis, diarrhea, and constipation (Horowitz and Chargaff, 1959; Elad, et al., 2020). 5-Fluorouracil (5-FU), an analog of uracil, is primarily used in the

✉ Jianzheng HE, hejianzheng1006@163.com
✉ Yongqi LIU, liuyongqi73@163.com
Yongqi LIU, https://orcid.org/0000-0003-2090-0017

Received July 7, 2025; Revision accepted Sept. 22, 2025;
Crosschecked xxx. xx, 20xx; Published online xxx. xx, 20xx

treatment of aerodigestive tract cancers and breast cancers, and is often accompanied by the development of IM (Horowitz and Chargaff, 1959; Lenfers et al., 1999). The potential mechanisms of IM are complex and remain unidentified. The condition involves oxidative stress, immune and inflammatory responses, and DNA damage (Elad, et al., 2020; Mohammed et al., 2023a). Currently, due to the complexity of its mechanism, IM is only managed using palliative coagents, including anti-inflammatories, biologic response modifiers, and antifungals (Mohammed et al., 2023b). Therefore, it is necessary to construct an efficient and accurate model to investigate the mechanisms of IM and related therapeutic agents.

Ferroptosis is a novel form of programmed cell death, distinct from apoptosis and necrosis, triggered by the iron-mediated accumulation of lipid peroxides (Stockwell, 2022). It plays a significant role in various intestinal diseases (Ru et al., 2024), such as chemotherapy-induced IM (Deng et al., 2021b; Ge et al., 2025), intestinal ischemia/reperfusion injury (Li et al., 2019), radiation-induced intestinal damage (Kong et al., 2023), and necrotizing enterocolitis (Teschke, 2024). The gut microbiota is a critical component of the intestinal barrier (Shi et al., 2017), and its dysbiosis is closely associated with the development and progression of chemotherapy-induced IM (Huang et al., 2022). Previous studies have indicated that the interaction between ferroptosis and the gut microbiota and its derived metabolites plays an important role in intestinal health and disease. For example, γ-aminobutyric acid (GABA), a microbial metabolite produced by the gut microbiota during metformin administration, alleviates liver ischemia/reperfusion injury by inhibiting ferroptosis (Wang et al., 2024a). Ginsenosides mitigate high-fat diet-induced non-alcoholic fatty liver disease by modulating the gut microbiota, reducing hepatic oxidative stress, lipid peroxidation, and ferroptosis (Liu et al., 2025). However, the microbiota-mediated role of ferroptosis in chemotherapy-induced IM remains unexplored and warrants further investigation.

While mice represent a classic model for studying chemotherapy-induced IM (Mohammed, et al., 2023a), they are limited by factors such as long experimental cycles and substantial economic costs. In recent years, *Drosophila melanogaster* has been widely used in intestinal disease research due to its structural and functional similarities to the human gut and high genetic homology (Lemaitre and Miguel-Aliaga, 2013; Wang et al., 2024b; Xiu et al., 2025). Structurally, the *Drosophila melanogaster* intestine consists of a chitinous peritrophic matrix (PM) and an underlying monolayer epithelial structure (Lemaitre and Miguel-Aliaga, 2013) that is similar to the physical protection provided by the mucus layer in the mammalian intestinal epithelium. In terms of function, similar to mammals, *Drosophila melanogaster* maintains intestinal homeostasis through the self-renewal and differentiation of intestinal stem cells (ISCs) (Lemaitre and Miguel-Aliaga, 2013; Jasper, 2020). Notably, the signaling pathways related to cell death and tissue regeneration are highly conserved between *Drosophila melanogaster* and humans (Bilak and Su, 2009; Lemaitre and Miguel-Aliaga, 2013), making *Drosophila melanogaster* an ideal model for studying intestinal diseases and hos-microbe interactions. Therefore, establishing a *Drosophila melanogaster* IM model can effectively facilitate mechanistic studying and drug screening.

In this study, a model of 5-FU-induced IM in *Drosophila melanogaster* was established first by assessing systemic toxicity, gastrointestinal tract dysfunction, intestinal damage, and epithelial cell death. Then, the molecular mechanism of 5-FU-induced IM was analyzed using a combination of transcriptomic, bioinformatic, and microbiome data. The significance of ferroptosis and gut microbiota was investigated using ferroptosis inhibitors, antibiotics (Abs), and fecal microbiota transplantation (FMT), which were validated in a mouse IM model. Overall, this study established a dual model of 5-FU-induced IM in flies, uncovered the crucial role of ferroptosis and gut microbiota in mediating 5-FU-induced IM, and provided novel insights for developing gut microbiota-based therapies against 5-FU-induced IM.

2 Materials and methods

2.1 Chemicals

5-Fluorouracil (5-FU, CAS: 51-21-8, 98%, Shanghai Yuanye Biotechnology Co., Ltd, China) was

dissolved in distilled water, and 1, 2.5, and 5 mmol/L of 5-FU were used in this study. Ferrostatin-1 (Fer-1, CAS:347174-05-4, MW: 262.35, 99.25 % purity, APExBIO, America) was dissolved in a 10 mmol/L stock solution, and 2.5, 5, and 10 μM of Fer-1 were used. Metronidazole (CAS:443-48-1, Assay: 99.0~101.0%, Sangon Biotech, China) and Carbenicillin (CAS:4800-94-6, Potency＞770 μg/mg, China) were dissolved in 15 mg/ml stock solutions stored at 4 °C, and 150 g/ml was used in the experiment. Tetracyclin (CAS: 64-75-5, Potency＞900 μg/mg, China) was dissolved in 7.5 mg/ml stock solutions stored at -20 °C, using 75 μg/mL.

2.2 Fly strains and rearing

Fly lines were as follows: w^{1118} (#5905) was obtained from the Bloomington Drosophila stock center (BDSC; Indiana, USA); *esg*-Gal4, UAS-GFP UAS-GFP were provided by Dr. Lihua Jin, Northeast Forestry University. *Myo1A*-GAL4, UAS-GFP were supplied by Dr. Rongwen Xi, NIBS, Beijing, China. All fly strains were nourished on standard agarose-cornmeal medium under conditions of 60% humidity at approximately 25 ◦C and a 12h light/12h dark cycle. For Abs treatment, female flies were fed with standard medium combined with 2.5 mmol/L 5-FU and mixed antibiotics (150 μg/mL metronidazole, 150 μg/mL metronidazole, and 75 μg/mL tetracyclin) (Chen et al., 2022). For Fer-1 treatment, female flies were fed with standard medium combining 2.5 mmol/L 5-FU and Fer-1 (2.5, 5, and 10 μM, respectively) (Xia et al., 2024b).

2.3 Development assay

The same number eggs of eggs of w^{1118} flies were inserted into vials equipped with standard food and 5-FU at 0, 0.01, and 0.025 mmol/L, respectively. The times at which eggs became pupae, pupae became adult flies, the number of pupae, and the percentage of eclosic flies were measured as described previously (He et al., 2022a). Third-instar larvae were transferred to the center of an agarose plate, their crawling trajectories were recorded for 1 minute, and their crawling velocity was calculated.

2.4 Survival rate assay

Two-to-four-day-old adult w^{1118} flies were separated by sex, with 20 females or males per vial. Fresh food was substituted every 3 days, and the number of dead flies was noted daily. The log-rank (Mantel-Cox) test was used to compare the difference in the survival curve.

2.5 Starvation resistance assay

Twenty adult males or females per vial were fed with 5-FU at 0, 1, 2.5, and 5 mmol/L, respectively, for 10 days, and were then transferred to vials containing 1% agarose. The number of dead flies was noted every 6 h until no live flies remained.

2.6 Fecundity and ovarian morphology experiments

Virgin females were collected from pinnipeds and allowed to mate overnight. They were then divided into groups of 20, transferred to fresh vials containing standard food, and maintained for 24 h. After this period, the number of eggs was recorded (Reiff et al., 2015). In addition, after being fed with 5-FU at 2.5 mmol/L for 2 days, ovaries were dissected in cold phosphate-buffered saline (PBS), and their morphology was examined using a stereomicroscope.

2.7 Food intake assay

Females were starved in empty vials for 18 h and then fed with food containing 2% sodium bromophenol blue for 4 h. Groups of 10 were scored based on the degree of abdominal coloration.

2.8 Excretion assay

Females were starved for 6 h and were then transferred in groups of 10 to 2 ml centrifuge tubes, where they were fed for 18 h through small holes in the walls and caps stained with medium. Then, the inner tube

wall was washed with PBS, and the mixed liquid was collected and measured at 625 nm using a microplate reader.

2.9 Crop motility assay

Flies, 10 per vial, were starved for 4 hours and then transferred to new vials containing blue-dyed food for an additional 4 hours. The flies' bodies were washed gently in PBS until no blue dye remained. Then, the intestines and crops were carefully separated and collected into two tubes containing PBS, respectively. The crops and intestines were ground in tubes until the dye was dissolved in the PBS. The absorbance of the mixed solution was measured at 625 nm using a microplate reader (Wei et al., 2020).

2.10 Intestine length assay

The flies' intestines were dissected in PBS, and measured.

2.11 Smurf assay

Females were maintained for 18 h in a dye-containing medium formulated with 5% sucrose, 2% Bromophenol blue sodium, and 1% agarose. Then, Smurf phenotypes were quantified. Specimens demonstrating visible dye diffusion beyond the digestive tract lumen were classified as Smurf-positive individuals (He et al., 2022a).

2.12 Intestinal acid-base homeostasis assay

Female flies were maintained for 4 h in the vial containing 1% agar and 1% Bromophenol blue sodium (Sigma, B5525), and the intestines were dissected and immediately scored (Li et al., 2023).

2.13 Trypan blue exclusion assay

The dissected intestines were soaked in 0.1% trypan blue for 20 min, washed in PBS, and scored immediately. The blue grade was detected from 0 (no color), 1 (baby blue), 2 (blue), to 3 (dark blue) (Wang, et al., 2024b).

2.14 MDA level measurement

The dissected intestines were collected from each group, homogenized, and then their malondialdehyde (MDA) levels were measured using the MDA Content Assay Kit (Cat: BC0025, Beijing Solarbio Science & Technology Co., Ltd.). The absorbance of samples was detected using a microplate spectrophotometer at 532 and 600 nm.

2.15 GSH activity measurement

Glutathione (GSH) activity was measured using the Reduced GSH Content Assay Kit G (Cat: BC1175, Beijing Solarbio Science & Technology Co., Ltd.). The absorbance of samples was detected using a microplate spectrophotometer at 412 nm.

2.16 Fe^{2+} level measurement

The Fe^{2+} level was measured using the Ferrous Ion Content Assay Kit (Cat: BC5415, Beijing Solarbio Science & Technology Co., Ltd.). The absorbance of samples was detected using a microplate spectrophotometer at 593 nm.

2.17 Ultrastructure of the epithelial cells

The ultrastructure of epithelial cells was examined using transmission electron microscopy (TEM). Briefly, the dissected midgut was postfixed, subjected to gradient ethanol dehydration, and then rinsed with acetone. Following embedding and polymerization, the samples were sectioned into ultrathin slices, stained

with lead citrate, and imaged using a TEM (Hitachi, HT7700).

2.18 Lipid peroxidation measurement

Lipid peroxidation was quantified using the BODIPY 581/591 C11 reagent (GLPBIO, #GC59145) according to established methodology (Xia et al., 2024a). The intestines were exposed to a 5 μM C11-BODIPY probe in darkness (37°C, 20 min), then washed three times with PBS prior to fluorescence microscopy analysis. Reduced (Ex/Em 581/591 nm) and oxidized (Ex/Em 488/510 nm) states were differentiated spectrometrically. Peroxidation indices were calculated using ImageJ by measuring the fluorescence intensity ratios between oxidized and reduced forms.

2.19 Histopathologic examination

Jejunum specimens were harvested and fixed overnight in 4% paraformaldehyde (PFA). Subsequently, the tissues were paraffin-embedded, sectioned at a thickness of 4 μm, and subjected to hematoxylin and eosin (H&E) staining

2.20 Immunohistochemistry and intestinal cells number measurement

Transgenic *Myo1a*-GFP and *esg*-GFP flies were used to quantify intestinal epithelial cells (IECs) and ISCs, respectively. Intestines were dissected in cold PBS, fixed in 4% PFA for 30 min, and washed with 0.3% triton-X in 1X PBS (PBST). Nuclei were stained with 4' 6-diamidino-2-phenylindole (DAPI). Reactive oxygen species (ROS) levels were assessed using Dihydroethidium (DHE) staining: dissected intestines were incubated with 30 μM DHE for 20 min, washed, fixed, and imaged. For anti-phospho-Histone H3 (pH3) staining, fixed midguts were incubated overnight with a rabbit anti-pH3 antibody, followed by 3 h with an Alexa 594 anti-rabbit antibody, DAPI staining, and imaging. For 7-aminoactinomycin D (7-AAD) staining, midguts were incubated with 30 μM 7-AAD for 15 min, washed, fixed, and imaged. Samples were mounted and imaged using an Olympus FV1000 confocal microscope. Fluorescence and numbers were analyzed using ImageJ.

Formalin-fixed, paraffin-embedded (FFPE) jejunum samples were sectioned onto Superfrost slides (Thermo Fisher Scientific), deparaffinized, and rehydrated following standard protocols. IHC was performed using an Autostainer (Dako Omnis, Agilent Technologies) with the following antibodies: anti-ASCL4 (Affinity, #DF15820), anti-Nrf2 (Affinity, #BF8017), anti-4-HNE (Abcam, #ab48506), and anti-GPX4 (Affinity, #DF6701).

2.21 Transcriptome analysis

Total RNA was isolated using TRIzol reagent (Thermo Fisher, #15596018) according to the manufacturer's protocol. Correlation and principal component analysis (PCA) were conducted using the princomp function in R (http://www.r-project.org/). Differential gene expression analysis was performed using DESeq2 for group comparisons and edgeR for sample comparisons. Genes with a false discovery rate (FDR) < 0.05 and an absolute fold change $\geqslant 2$ were defined as differentially expressed. A functional enrichment analysis of gene ontology (GO) terms and kyoto encyclopedia of genes and genomes (KEGG) pathways was performed on the differentially expressed genes.

2.22 Bioinformatics and potential targets analysis

The GSE28873 dataset, obtained from the National Center for Biotechnology Information (NCBI), comprises transcriptional profiles of three samples from mice with 5-FU-induced intestinal damage and six healthy controls. Differential gene expression in the 5-FU-treated and control groups was compared using the 'GEOquery', 'limma', and 'umap' packages in R. A Venn diagram was used to identify overlapping genes between GSE28873 and transcriptomic data. Functional annotation of these genes, including GO biological processes and KEGG pathways, was performed using the DAVID online tool (https://david.ncifcrf.gov/).

Ferroptosis-related genes were identified from the intersected targets using the FerrDB database (http://www.zhounan.org/ferrdb). Key pathways associated with hub genes were analyzed using KEGG pathway analysis, and a protein-protein interaction (PPI) network of ferroptosis-related genes was constructed using the GeneMANIA Web Server (https://genemania.org).

2.23 16S rRNA gene sequencing analysis

The raw sequencing data, in FASTQ format, underwent adapter trimming and quality control. Paired-end reads were processed through DADA2 for quality filtering, error correction, read merging, and chimera removal. Amplicon sequence variants (ASVs) were identified using QIIME 2, with representative sequences taxonomically classified against the SILVA v138 (16S/18S rRNA) and UNITE (ITS) databases via the q2-feature-classifier plugin. Alpha diversity was evaluated using Chao1 richness and Shannon diversity indices. Beta diversity was assessed using unweighted UniFrac distance-based principal coordinates analysis (PCoA) and phylogenetic tree reconstruction. All 16S rRNA gene amplicon sequencing and bioinformatics analyses were conducted by OE Biotech Co., Ltd (Shanghai, China).

2.24 RT- PCR analysis

Total RNA was isolated from dissected female guts using Trizol reagent (Invitrogen) and reverse-transcribed into complementary DNA (cDNA) using Hieff® reverse transcriptase (YEASEN, Shanghai, China). Reverse transcription-polymerase chain reaction (RT-PCR) was conducted using the GFX 96 Connect™ Optics Module (Bio-Rad Laboratories) according to the manufacturer's protocol for Multiplex PCR Master Mix (YEASEN, Shanghai, China). Primer sequences are listed in Table 1; mRNA levels were normalized to the internal control *RP49*; and relative quantification was calculated using the $2^{-\Delta\Delta Ct}$ method.

Table1 List of forward and reverse primers.

Genes	Forward	Reverse
Tsf1	CTATCGCGTGATCTCTGAGATCC	CTTCAGGACGTGCGTGTTCTTCAG
Fer1HCH	CCCTGGCTGTTCCTGAGA	TACTGGTAGGAGGCGTTGAT
Mvl	AAGACTGGGCGTGGTTACAG	TCCACAGTATCCAACGTGGC
PGRP-SD	ACTTGGATCGGTTTGCTCATC	AGGGAGTTTCCATGCTGTCTAT
PGRP-LC	AAACGATCCGTTGACTGGAC	TACGCTTGGATTCCGTTTTC
PGRP-SA	TCAATGCGGAGTTGAACTGGGAGA	TAGAGTTTCAGTCCAGGGCTGCTT
Mtk	GCAACTTAATCTTGGAGCGA	CGGTCTTGGTTGGTTAGGAT
AttA	ACAAGCATCCTAATCGTGGC	TCAGATCCAAACGAGCATCAG
Dif	ATGTTTGAGGAGGCTTTCGG	GAACCGGCGGTGCGACCCTCGC
Def	GTTCTTCGTTCTCGTGG	CTTTGAACCCCTTGGC
Drs	CGTGAGAACCTTTTCCAATAYGATG	TCCCAGGACCAGCAT
Mco3	GCAACAAGAGCTCCCTGGCCG	GCTCCTGAATATTGCGCAAATCG
DUOX	GCCGAGGGAGCAGATAAATCA	TCTTCATGACACTCGGCACC
HO	ATGTCAGCGAGCGAAGAAACA	TGGCTTTACGCAACTCCTTTG
cnc (Nrf2)	GAGGTGGAAATCGGAGATGA	CTGCTTGTAGAGCACCTCAGC
Keap1	CAAGGAGTCGGAGATGTCG	GTAGAGGATGCGTGACATGG
Sod	GCGGCGTTATTGGCATTG	ACTAACAGACCACAGGCTATG
gstd1	TGATCAATCAGCGCCTGTACT	GCAATGTCGGCTACGGTAAG
RP49	CTTCATCCGCCACCAGTC	GCACCAGGAACTTCTTGAATC

Tsf1, transferrin 1; *Fer1HCH*, ferritin 1 heavy chain homologue; *Mvl*, malvolio; *PGRP-SD*, peptidoglycan recognition protein SD; *PGRP-LC*, peptidoglycan recognition protein LC; *PGRP-SA*, peptidoglycan recognition protein SA; *Mtk*, metchnikowin; *AttA*: attacin-A; *Dif*, dorsal-related immunity factor; *Def*, defensin; *Drs*, drosomycin; *Mco3*, multicopper oxidase 3; *DUOX*, dual oxidase; *H0*, heme oxygenase; *cnc*, cap-n-collar; *Keap1*, kelch-like ECH-associated protein 1; *sod*, superoxide dismutase; *gstd1*, glutathione S transferase D1; *RP49*, ribosomal protein L32.

2.25 Mice and induction of chemotherapy-induced intestinal mucositis

The mouse protocols were approved by the Institutional Animal Care and Use Committee of Gansu University of Chinese Medicine (approval number: SY2024-264), conducted in compliance with their

guidelines and the GB/T 35892-2018 Guidelines for Ethical Review of Laboratory Animal Welfare.

Six-week-old C57BL/6 female mice were purchased from Sibeifu (Beijing) Biotechnology Ltd. All animals were housed in a specific pathogen-free (SPF) facility at Gansu University of Chinese Medicine under a 12 h light/dark cycle, with access to a standard chow diet and water ad libitum. Mice were randomly and evenly allocated into control and model groups, with eight mice per group. Model mice were intravenously injected with 5-FU (75 mg/kg/day) every 24 h from day 1 to day 4, and control mice received intravenous physiological saline as the vehicle.

2.26 FMT experiment

FMT was performed using an established protocol (Wei et al., 2023). Flies fed 2.5 mmol/L 5-FU received FMT from either control donors or 5-FU donors, and were designated 5-FU + FMT of the control groups and 5-FU + FMT of the 5-FU groups, respectively, while flies fed a standard diet received FMT from control or 5-FU donors and were designated 5-FU + FMT of the control groups and 5-FU + FMT of the 5-FU groups, respectively. Here, FMT of 5-FU refers to culturing flies in fecal-conditioned medium derived from flies treated with 5-FU for 10 d, and FMT of control refers to culturing flies in FMT derived from flies treated with a standard diet for 10 d.

2.27 Statistical analysis

All experiments were conducted with a minimum of three replicates. Data are presented as means ± standard error of the mean (SEM). The Log-rank test was applied to assess the statistical significance of survival rates across groups. A one-way ANOVA was utilized for comparisons involving three or more groups, while the unpaired Student's t-test was employed for comparisons between two groups. Statistical analyses were performed using GraphPad Prism version 8.0.2. Statistical significance levels are denoted by $*p < 0.05$, $**p < 0.01$, and $***p < 0.001$.

3. Results

3.1 Exposure to 5-FU induces systemic side effects in flies

The survival rates and anti-starvation ability of flies fed with 5-FU at 0, 1, 2.5, and 5 mmol/L were measured to determine whether 5-FU had side effects on adult flies. 5-FU administration considerably shortened the survival rate in both females and males in a dose-dependent way (Figs. 1a and 1b). Furthermore, supplementation of 5-FU decreased the survival rate under starvation in both females and males, indicating that 5-FU led to a reduced capacity to tolerate stress (Figs. 1c and 1d). To assess the fertility side effect on females, the number of eggs laid was calculated when females were treated with 5-FU at 0, 1, and 2.5 mmol/L for 1, 2, and 3 days, respectively. Interestingly, the number of eggs laid in 24 h significantly diminished (Fig. 1e). Specifically, administration of 5-FU at 2.5 mmol/L for 2 days could lead to significant atrophy of ovarian morphology (Fig. 1f). To investigate the potential developmental toxicity of 5-FU on flies, the eggs were treated with 5-FU at 0, 0.01, and 0.025 mmol/L. Intake of 5-FU delayed the duration from egg to pupa, decreased the number of pupae and the area of pupa, and damaged the crawl ability of third instar larvae, which was dose-dependent (Figs. 1g-1j). Furthermore, 0.01 mmol/L 5-FU supplementation remarkably decreased the rate of eclosion and extended eclosion time (Figs. 1k and 1l). Thus, these results indicated that 5-FU had a serious, systemic toxic effect in flies.

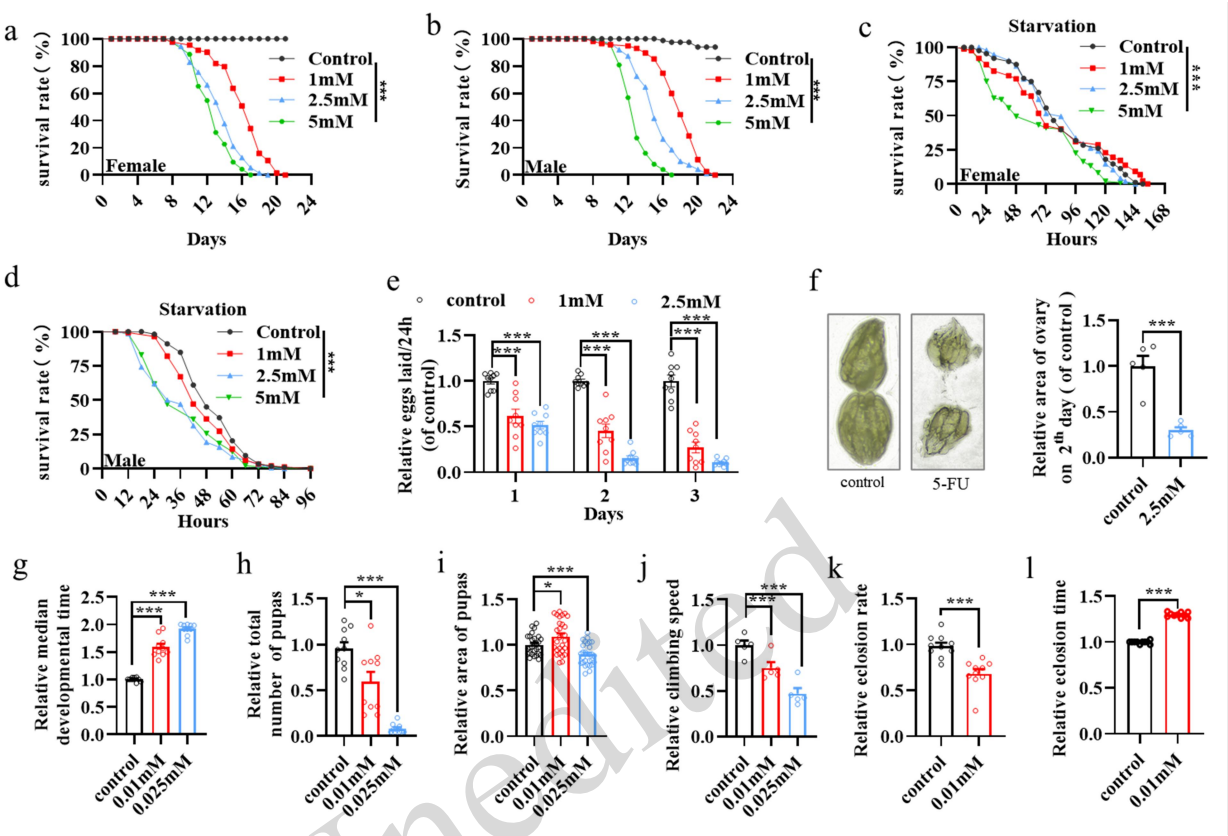

Fig.1 Exposure to 5-FU induces systemic side effects in flies.

(a, b) Survival rate of females (n=115–125) and males (n=115–132). (c, d) Anti-starvation survival rate of females (n=88–97) and males (n=113–136). (e) Relative numbers of eggs laid number in 24 h for females fed with 5-FU at 1 and 2.5 mmol/L for 1, 2, and 3 d (n=9). (f) The morphology and relative area of the ovary in females fed with 5-FU at 2.5 mmol/L for 2 d (n=5). (g) The relative median development time (n=10). (h) The relative total number of pupae (n=10). (i) The relative area of pupae (n=28). (j) The relative climbing speed of larvae after flies' eggs were treated with 5-FU (n=6). (k) The relative eclosion rate (n=10). (l) Relative eclosion time (n=10). 5-FU, 5-fluorouracil. Data are presented as mean ± SEM, two-sided unpaired t-tests with Welch's correction; *$p < 0.05$ and ***$p < 0.001$.

3.2 Exposure to 5-FU induces gastrointestinal tract dysfunction in flies

To explore whether 5-FU had a side effect on the gastrointestinal tract of flies, the food intake, excretion, crop motility, intestine length, "Smurf", and intestinal acid-base homeostasis of females were measured. Administration of 5-FU significantly increased the food intake and decreased the excretion in females in a dose-dependent manner (Figs. 2a and 2b), indicating that the ingested food was not digested in time. To further explore the reason for food accumulation in the gastrointestinal tract, a crop motility assay was carried out. Interestingly, 2.5 mmol/L 5-FU increased the dye of the crop, decreased the dye of the intestine, and induced an inverted "crop/intestine" dye ratio, indicating typical gastrointestinal tract dysfunction (Figs. 2c-2e). In addition, supplementation with 5-FU significantly shortened intestinal length and induced an increased ratio of "Smurfs", meaning increased intestinal permeability (Figs. 2f and 2g). Additionally, an imbalanced gastrointestinal acid-based homeostasis was observed after treatment with 5-FU (Fig. 2h). Above all, these results indicated typical gastrointestinal tract dysfunction in flies exposed to 5-FU.

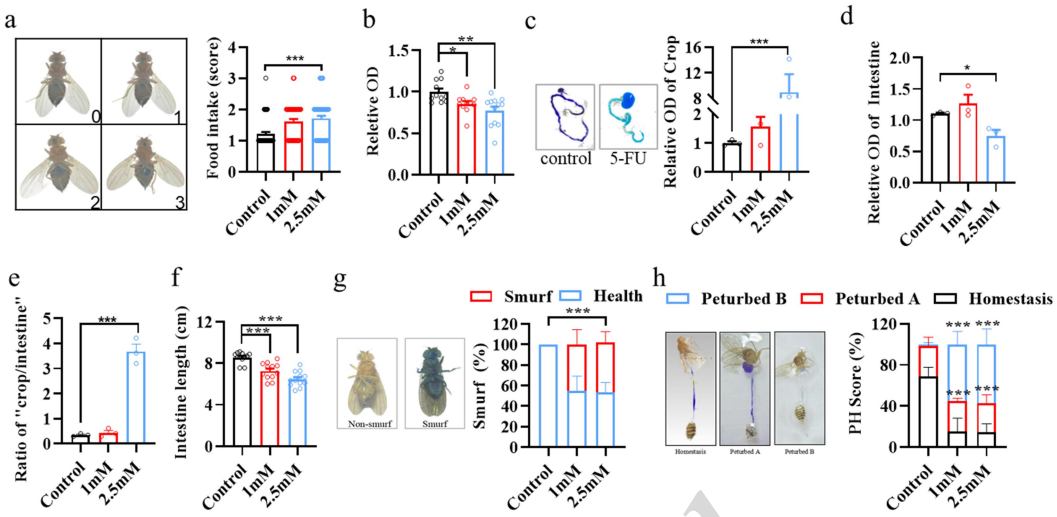

Fig.2. Exposure to 5-FU induces gastrointestinal tract dysfunction and intestinal damage in flies.

(a) Abdominal scoring criteria and food intake (n=64–66). (b) Excretion (n>18). (c, d) Food storage capacity of crop and intestine (n=3). (e) Ratio of food storage capacity between crop and intestine (n=3). (f) Intestine length (n=12–13). (g) Typical images and percentage of "Smurfs" (n=3). (h) Typical images and quantification of intestine of females fed with the pH indicator Bromophenol Blue, which has three types of gastrointestinal tract, including "Homeostasis", "Perturbed A", and "Perturbed B" (n=4). Data are presented as mean ± SEM, two-sided unpaired t-tests with Welch's correction; *$p < 0.05$, **$p < 0.01$, ***$p < 0.001$.

3.3 Exposure to 5-FU induces intestinal cell damage and decreases the proliferation of intestinal stem cells in flies

To investigate whether 5-FU induces intestinal cell damage, the extent of intestinal cell death and changes in intestinal epithelial substructure were detected. 5-FU administration significantly induced massive cell damage in a dose-dependent manner (Fig. 3a and 3b). The 2.5 mmol/L 5-FU supplementation damaged the ultrastructure of IECs, in which the microvilli were sparse, truncated, and caducous (Figs. 3c-3d). IECs were the most predominant type of intestinal cell, maintaining the intestinal functions of acting as a barrier and facilitating nutrient absorption (Peterson and Artis, 2014). To detect epithelial cell impairment, *Myo1A*-GFP flies with specific labeling of IECs and 7-AAD staining were used. Administration of 5-FU at 2.5 mmol/L resulted in a significant decrease in the fluorescence intensity of GFP-positive cells and a remarkable increase in 7-AAD-positive cells in the midgut (Figs. 3e-3g), indicating severe cell death in IECs. The ISCs' proliferation ability was then assessed via the *esg*-GFP flies and a PH3 assay. Administration of 2.5 mmol/L 5-FU significantly decreased the number of GFP-positive cells in the midgut and noticeably reduced the PH3-positive cells (Figs. 3e, 3h and 3i), indicating a significant reduction of ISCs' proliferation. Thus, 5-FU may induce intestinal cell damage and decrease ISC proliferation in adult flies.

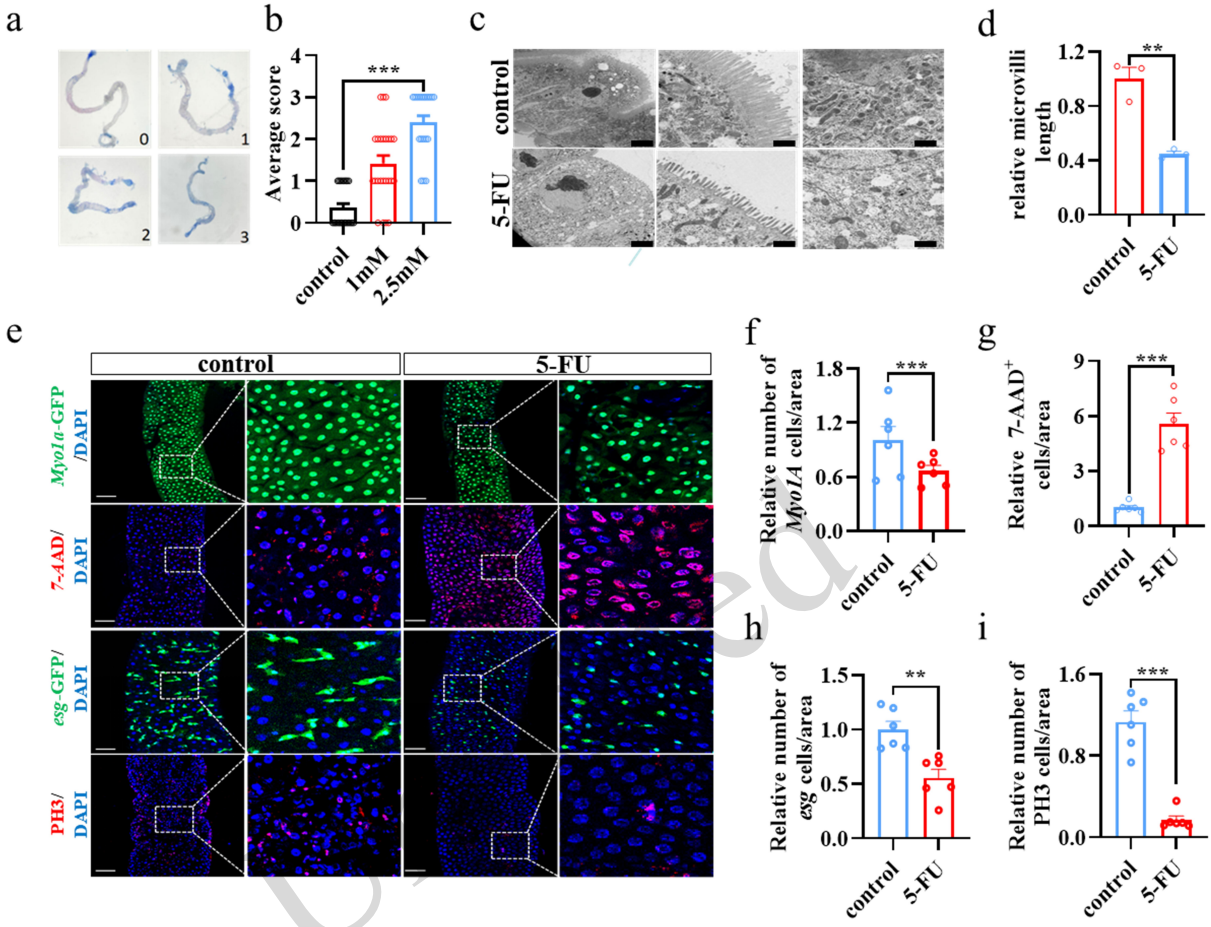

Fig.3 Exposure to 5-FU induces intestinal cell damage and decreases the proliferation of intestine stem cells in flies. (a, b) Trypan Blue experiment scoring criteria and quantization (n=23–25). (c) Transmission electron microscopy of intestinal epithelial cells. Intestinal epithelial cell with magnification: 1500×, 7000×, and 15000×. Nu, Mv, and M are abbreviations for nucleus, micro villi, and mitochondria, respectively. (d) The relative length of microvilli of intestinal epithelial cells (n=3). (e) The representative images of midguts from *Myo1a*-GFP, *esg*-GFP flies, and 7-aminoactinomycin D (7-AAD), anti-phospho-Histone H3 (PH3) assay. (F) Quantification of the amounts of cells (*Myo1a*-GFP positive) in the experiment (n=6). (g) Quantification of epithelial cell death via 7-AAD assay (n=6). (h) Quantification of the amounts of cells (*esg*-GFP positive) in the experiment (n=6). (i) Quantification of proliferation of intestinal stem cells (ISCs) via PH3 assay (n=6). Data are presented as mean ± SEM, two-sided unpaired t-tests with Welch's correction; $*p < 0.05$, $**p < 0.01$, $***p < 0.001$.

3.4 The intestinal injury caused by 5-FU is associated with various signaling pathways

To explore the potential molecular networks of 5-FU-induced intestinal damage, total intestine RNA, isolated from flies fed with 2.5 mmol/L 5-FU for 10 days, was sequenced. PCA revealed distinct clustering between the two groups (Fig. 4a). A volcano plot demonstrated the differently expressed levels of 19,142 genes, including 1262 up-regulated genes and 1079 downregulated genes (Fig. 4b). A heat map was created to exhibit the genes that most significantly differed between the control and model groups (Fig. 4c). To determine the biological functions and signal pathways, GO and KEGG enrichment were carried out, revealing that 12 significant pathway terms and correlated pathways were listed, including the fatty acid metabolic process, fatty acid β-oxidation, and the immune response (Figs. 4d and 4f). To delve deeper into the potential mechanisms of 5-FU-induced IM, a combined bioinformatics and transcriptomics analysis was conducted. The gene expression profiles (GSE28873) were analyzed using the GEO2R tool, with no obvious outlier samples (Fig. 4f). This analysis examined 29,922 genes, in which 311 were upregulated and 364 were

downregulated (Fig. 4g). Then, a Venn analysis illustrated the overlap of 7803 differential genes identified via bioinformatics and transcriptomics, which were key differential genes involved in the 5-FU-induced IM (Fig. 4h). Then, 447 significant GO terms and 65 KEGG terms were identified, pointing to various signal pathways, including ferroptosis and the immune system (Figs. 4i and 4j).

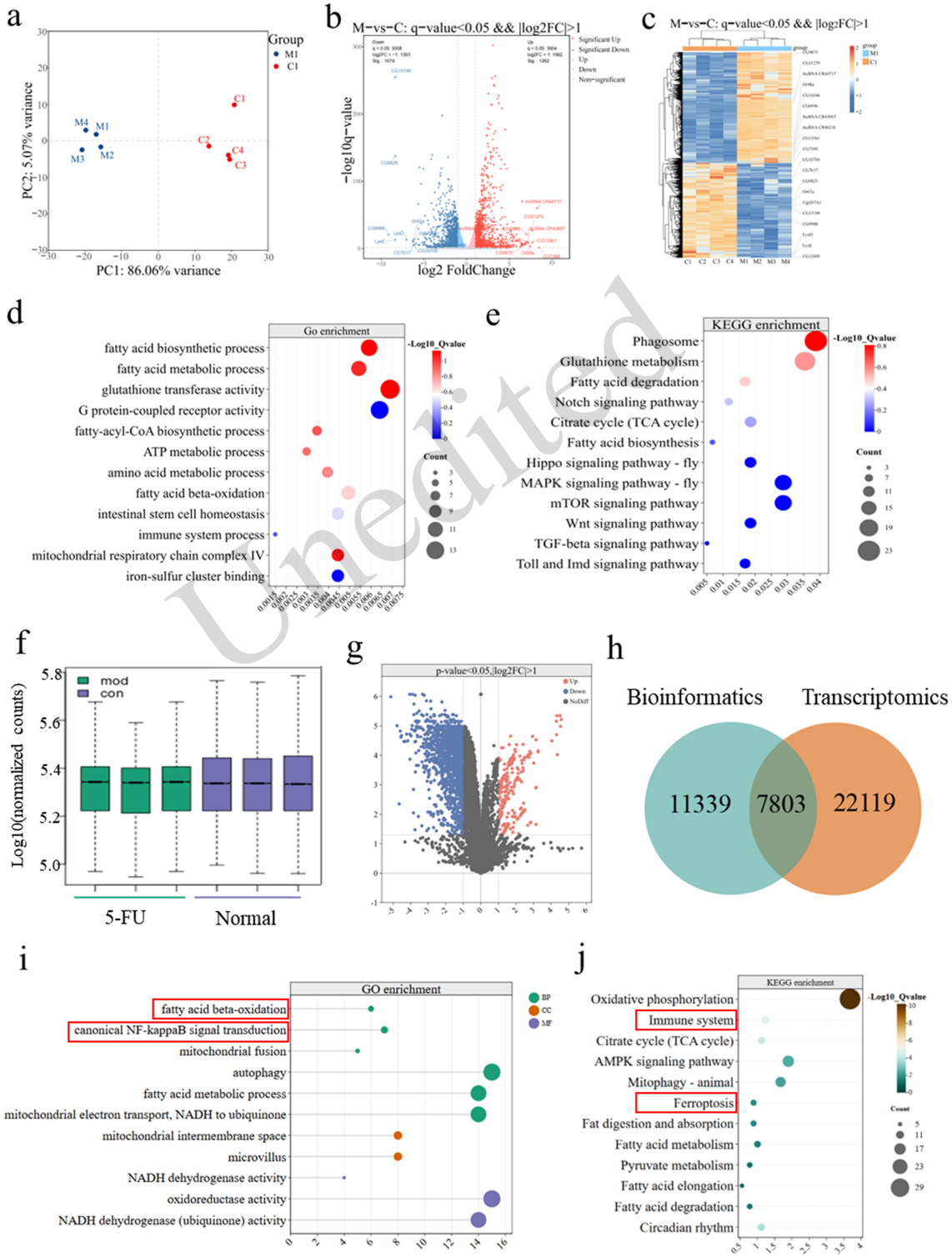

Fig.4 Bioinformatics combined with transcriptomics analysis of 5-FU-treated and control groups.

(a) A PCA plot is used to cluster samples, revealing good repeatability. Each point represents one sample; percentages denote contribution ratios. (b) A volcano plot of DEGs. Compared to genes in the control group, up-regulated and down-regulated genes in 5-FU-treated samples are marked as red and blue points, respectively; while non-significant genes are shown in gray. (c) A heatmap of the top significantly ($p < 0.05$) DEGs identified. (d) GO enrichment analysis of the 5-FU-treated and control groups. (e) KEGG enrichment analysis of the 5-FU-treated and control groups. (f) Box plot of 5-FU-treated rat versus normal rat gastrointestinal tissue analysis. (g) Volcanic map of all the genes in GSE28873. (h) DEGs Venn diagram from the bioinformatics data mining and transcriptomics; 7803 represents the targets of 5-FU-induced intestinal injury. (i and j) KEGG and GO functional enrichment analysis of hub DEGs. PCA, principal components analysis; DEGs, differentially expressed genes; GO, gene ontology; KEGG, kyoto encyclopedia of genes and genomes.

3.5 5-FU induced gut microbiota dysbiosis is associated with ferroptosis in flies

To characterize the profile of gut microbiota after 5-FU exposure, the gut microbiota of flies fed with 2.5 mmol/L 5-FU for 10 d were sequenced. PCoA reflected a significant separation between two groups (Fig. 5a). Furthermore, compared to the control group, the 5-FU group exhibited lower Shannon, Chao1, and Simpson indices, indicating a significant decrease in species diversity post 5-FU exposure (Fig. 5b). In addition, at the family level, 5-FU exposure markedly reduced the relative abundance of *Orbaceae* and *Lactobacillacea*, and increased the relative abundance of *Enterobacteriaceae* and *Acetobacteraceae* (Fig. 5c). At the genus level, administration of 5-FU significantly reduced the relative abundance of *Lactobacillus*, and increased the relative abundance of *Acetobacter* (Fig. 5d). For the spices level, 5-FU supplementation significantly reduced the relative abundance of *Lactobacillus,* increased the relative abundance of *Acetobacter_pasteurianus,* and decreased the relative abundance of *Lactobacillus_plantarum* (Fig. 5e). Linear discriminant analysis (LDA) effect size (LEfSe) identified *Proteobacteria* as a biomarker that distinguished the 5-FU from the control (Fig. 5f).

To clarify the correlation between gut microbiota and ferroptosis and immune response, a Spearman's correlation analysis was performed. The results showed that ferroptosis and immune response are positively correlated with the abundance of *Proteobacteria*, and negatively correlated with the abundance of bacteria belonging to the *Firmicutes* phylum and the *Lactobacillacea* family (Fig. 5g). Additionaly, the bacteria included in Spearman's correlation analysis were counted. Interestingly, 5-FU exposure increased the abundance of pathogen-associated bacteria *Proteobacteria*; however, it decreased the abundance of *Firmicutes*, *Lachnospiraceae*, *Sutterellaceae*, *Orbaceae*, *Lachnospiraceae_NK4A136_group*, and *Alistipes*, *[Eubacterium]_coprostanoligenes_group* (Figs. 5h-5l). Overall, these results suggested that 5-FU-induced gut microbiota dysbiosis was associated with ferroptosis and innate immune response.

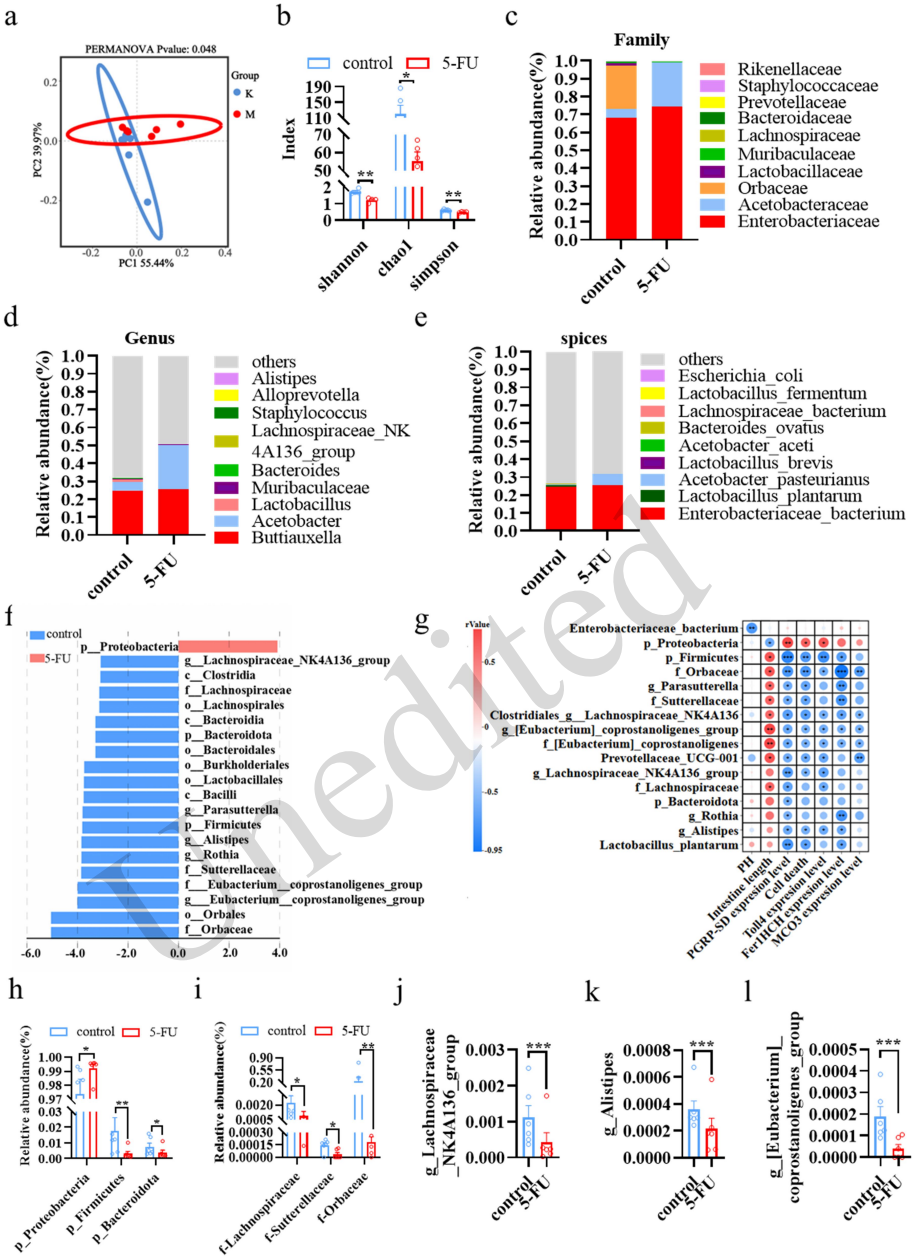

Fig.5 Exposure to 5-FU-induced gut microbiota dysbiosis is associated with intestinal injury, ferroptosis, and immune response.

Fecal microbiota composition was analyzed using 16S rRNA gene sequencing (n=6). (a) Principal co-ordinate analysis of Bray distance (p-value from Anosim analysis is shown). (b) Shannon, chao1 and Simpson index. (c) Composition abundance of the bacterial family. (d) Composition abundance of the bacterial genus. (e) Composition abundance of the bacterial species. (f) LEfSe showing the most differentially significant abundant taxa enriched in microbiota. (g) Spearman's correlation among the effects of 5-FU on gut microbiota, PH, intestine length, cell death and the mRNA expression of peptidoglycan recognition protein SD (*PGRP-SD*), Ferritin 1 heavy chain homolog (*Fer1HCH*), and multicopper oxidase 3 (*Mco3*). (h) Relative abundance of the 5-FU-induced bacterial phylum in the control and 5-FU groups. (i) Relative abundance of 5-FU-induced bacteria families in the control and 5-FU groups. (i-k) Relative abundance of 5-FU-induced bacterial genus in the control and 5-FU groups. Data are presented as mean ± SEM, two-sided unpaired t-tests with Welch's correction; *$p < 0.05$, **$p < 0.01$, ***$p < 0.001$.

3.6 Exposure to 5-FU induces intestinal injury via ferroptosis in the intestine of flies

To identify potential human gene targets involved in the impact of 5-FU on the intestine, the ferroptosis pathway was detected. The FerrDB database and Venn analysis were used to identify genes involved in the effects of 5-FU exposure-induced ferroptosis on the intestine. The analysis identified 205 potential ferroptosis-related genes, including long-chain acyl-CoA synthetase 4 (*ACSL4*), kelch-like ECH-associated protein 1 (*Keap1*), toll-like receptor 4 (*TLR4*), and solute carrier family 7 member 11 (*SLC7A11*) (Fig. 6a). Then, KEGG enrichment of the 205 identified hub genes showed that ferroptosis and toll-like receptor signal pathway were in the top 20 (Fig. 6b). The PPI network further highlighted the importance of *ACSL4*, *Keap1*, *TLR4*, and *SLC7A11* in the pathophysiology of 5-FU-induced IM (Fig. 6c). These results indicated that ferroptosis was engaged in 5-FU induced intestine injury.

To further elucidate the role of ferroptosis in 5-FU-induced intestinal injury, key ferroptosis markers, including iron levels, ROS levels, and lipid peroxidation levels were assessed. Compared to the control, 5-FU significantly increased the ROS level, MDA activity, total iron levels, and ox/non-ox ratio, while decreasing GSH activity (Figs. 6d-6h). To understand the molecular mechanisms underlying ferroptosis in 5-FU-induced injury, the expression of genes linked to iron metabolism and the oxidation-reduction system was examined. The results showed that 5-FU exposure resulted in an abnormal increase of multicopper oxidase 3 (*Mco3*), dual oxidase (*DUOX*), and heme oxygenase (*HO*), which can cause a high level of ROS and peroxidized iron in the intestine (Fig. 6i). Furthermore, exposure to 5-FU increased the expression of Malvolio (*Mvl*), also known as Divalent Metal Transporter-1 (*DMT1*), the primary iron importer (Orgad et al., 1998; Bettedi et al., 2011) (Fig. 6j). Additionally, it promoted the expression of Ferritin 1 heavy chain homolog (*Fer1HCH*), which exhibited the ferroxidase activity required for iron loading (Mandilaras et al., 2013) (Fig. 6j). However, the expression of *Tsf1*, required for septate junction assembly in epithelial cells, was reduced (Fig. 6j), and the expression of *Nuclear factor erythroid 2-related factor 2* (*Nrf2)*, *Keap1*, superoxide dismutase (*sod*), and glutathione S transferase D1 (*gstd1*) was significantly decreased, suggesting an abnormal inhibition of the *Nrf2* signal pathway after 5-FU treatment (Fig. 6k). To further confirm the hypothesis, we assessed the survival rate and intestinal length following Fer-1 treatment. Administration of Fer-1 showed a significant increase in survival rate and intestinal length (Figs. 6l-6m). Thus, our results showed that the inhibition of ferroptosis alleviated 5-FU-induced IM, which was a novel therapy target.

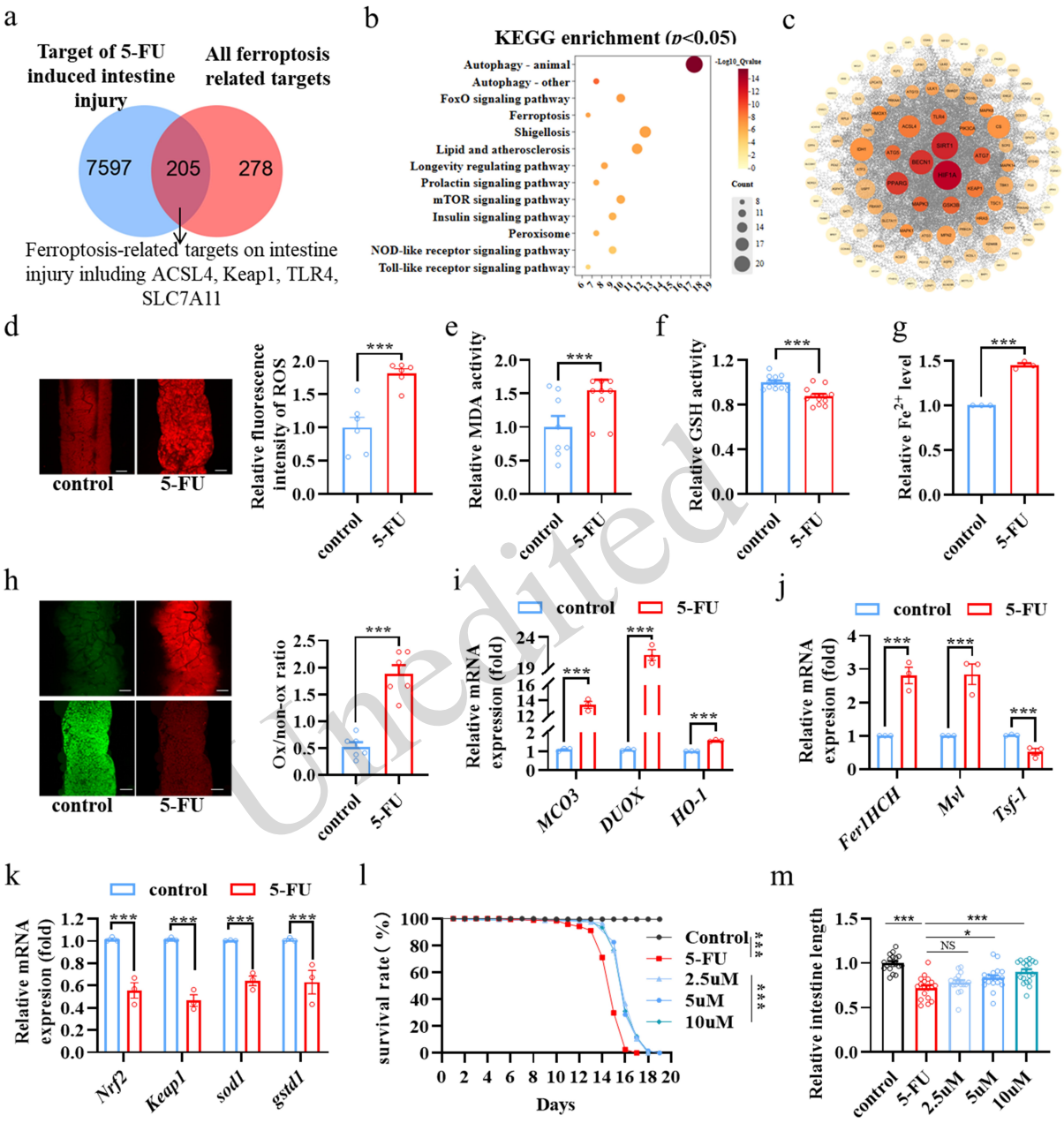

Fig.6 Exposure to 5-FU induces intestinal damage via activating ferroptosis in flies.

(a) A Venn diagram between the hub genes of bioinformatics data mining and transcriptomics, and ferroptosis-related targets. (b) The KEGG enrichment analysis of the ferroptosis-related targets on 5-FU-induced intestinal injury. (c) The PPI analysis of 205 genes. (d) The ROS level (n=6). (e) The relative GSH activity (n=3). (f) The relative MDA activity (n=3). (g) The relative Fe^{2+} level (n=3). (h) Accumulation of lipid peroxides by using BODIPY C11 probe (n=6). (i) The relative mRNA expression level of *Mco3*, *DUOX* and *HO* (n=3). (j) The relative mRNA expression level of *Fer1HCH*, *Mvl* and *Tsf-1* (n=3). (k) The relative mRNA expression level of *Nrf2*, *Keap1*, *sod* and *gstd1* (n=3). (l) The survival rate of females fed without or with Fer-1 (n=180). (m) The survival intestine length of females fed without or with Fer-1 (n=16). KEGG, kyoto encyclopedia of genes and genomes; PPI, protein-protein interaction; ROS, reactive oxygen species; GSH, glutathione; MDA, malondialdehyde; *Tsf1*, transferrin 1; *Fer1HCH*, ferritin 1 heavy chain homologue; *Mvl*, malvolio; *Mco3*, multicopper oxidase 3; *DUOX*, dual oxidase; *HO*, heme oxygenase; Nrf2, *Nuclear factor erythroid 2-related factor 2*; *Keap1*, kelch-like ECH-associated protein 1; *sod*, superoxide dismutase; *gstd1*, glutathione S transferase D1. Data are presented as mean ± SEM, two-sided unpaired t-tests with Welch's correction; *$p < 0.05$, **$p < 0.01$, ***$p < 0.001$.

3.7 Elimination of gut microbiota ameliorates 5-FU-induced IM, ferroptosis, and innate immune response

To identify the role of gut microbiota-mediated ferroptosis and immune response in 5-FU-induced IM, Abs treatment was used to eliminate gut microbiota in 5-FU-fed flies (Fig. 7a). The gut microbiota disorders-indiced activation of the innate immune response, and the relationship between gut microbiota and innate immune response was depicted in Fig. 7b. Administration of Abs significantly increased the survival rate, relieved intestinal length, and disturbed acid-based homeostasis in 5-FU treated flies (Figs. 7c-7e). Next, we determined whether gut microbiota dysregulation promotes 5-FU-induced IM via activating the Toll and IMD signal pathway. Compared to the 5-FU group, the mRNA expression of peptidoglycan recognition protein SA (*PGRP-SA*), peptidoglycan recognition protein SD (*PGRP-SD*), and peptidoglycan recognition protein LC (*PGRP-LC*), that bind to bacterial Lysine-type peptidoglycans (PGNs) and fungal β-(1,3)-glucan and trigger Toll-NF-kB and IMD-NF-kB signaling (Iatsenko et al., 2016), was significantly decreased following Abs administration (Fig. 7f). Subsequently, the mRNA levels of *Def*, *Dif*, and *Drs* (homologues of *NF-kB*) showed a striking reduction when fed with Abs (Fig. 7g). In addition, supplementation with Abs decreased the mRNA expression levels of antimicrobial peptides (AMPs) relative genes *AttA* and *MtK* in 5-FU-treated flies (Fig. 7h). Furthermore, to investigate whether gut microbiota-induced intestinal damage involves ferroptosis, the related ferroptosis indicators were examined. Administration of Abs reduced the mRNA expression of *Mco3*, *Fer1HCH*, and *Mvl*, the relative activity of MDA, and the relative level of Fe^{2+} in 5-FU-treated flies (Figs. 7i-7k). In addition, supplementation with Abs increased the relative activity of GSH (Fig. 7l). Taken together, these results indicated that Abs treatment can alleviate 5-FU induced IM by inhibiting ferroptosis and the immune response.

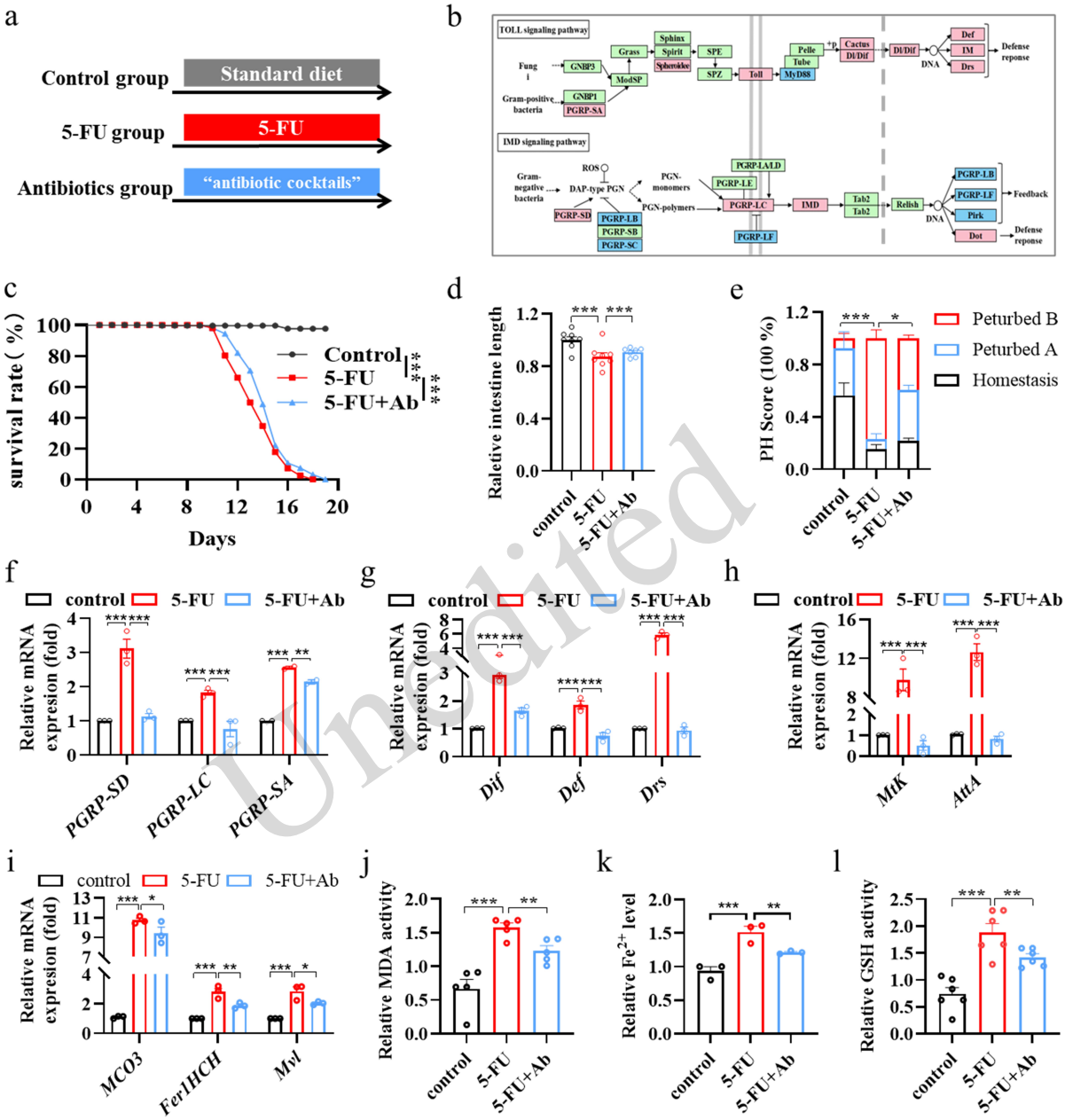

Fig.7 Elimination of gut microbiota ameliorates 5-FU-induced IM via inhibiting ferroptosis and the innate immune response in flies.

(a) Schematic timeline for the model establishment of the control, 5-FU, and 5-FU+Abs group. Females were fed with a standard diet, a standard diet combing 5-FU, and a standard diet combining 5-FU and antibiotics for 10 d. (b) Toll and IMD signaling pathway. (c) The survival rate (n=180). (d) The intestine length (n=16). (e) The PH score (n=3). (f) The mRNA expression level of *PGRP-SG*, *PGRP-LC*, and *PGRP-SA* (n=3). (g) The mRNA expression level of *Dif*, *Def*, and *Drs* (n=3). (h) The mRNA expression level of *Mtk* and *AttA* (n=3). (i) The mRNA expression level of *Mco3*, *Fer1HCH*, and *Mvl* (n=3). (j) The relative MDA activity (n=5). (k) The relative Fe^{2+} activity (n=3). (l) The relative GSH activity (n=6). 5-FU, 5-fluorouracil; Abs, antibiotics; *PGRP-SD*, peptidoglycan recognition protein SD; *PGRP-LC*, peptidoglycan recognition protein LC; *PGRP-SA*, peptidoglycan recognition protein SA; *Mtk*, metchnikowin; *AttA*, attacin-A; *Dif*, dorsal-related immunity factor; *Def*, defensin; *Drs*, drosomycin. Data are presented as mean ± SEM, two-sided unpaired t-tests with Welch's correction; *$p < 0.05$, **$p < 0.01$, ***$p < 0.001$.

3.8 Gut microbiota dysbiosis contributes to 5-FU-induced intestinal damage in flies

To further elucidate the causal relationship between gut microbiota dysbiosis and 5-FU-induced IM, we transplanted the fecal microbiota from control group flies and 5-FU-treated group flies into standard diet-fed flies and 5-FU-fed flies, respectively (Fig. 8a). Compared to flies receiving microbiota from the 5-FU group, transplantation of microbiota from the control group enhanced the survival rate, increased intestinal length, and improved intestinal acid-base homeostasis in 5-FU-treated flies (Figs. 8b, 8d, and 8f). Conversely, transplantation of microbiota from the 5-FU group into standard diet-fed flies reduced survival rate, shortened intestinal length, and disrupted intestinal acid-base homeostasis (Figs. 8c, 8e and 8g). These results demonstrated that gut microbiota dysbiosis contributes to 5-FU-induced intestinal damage in flies.

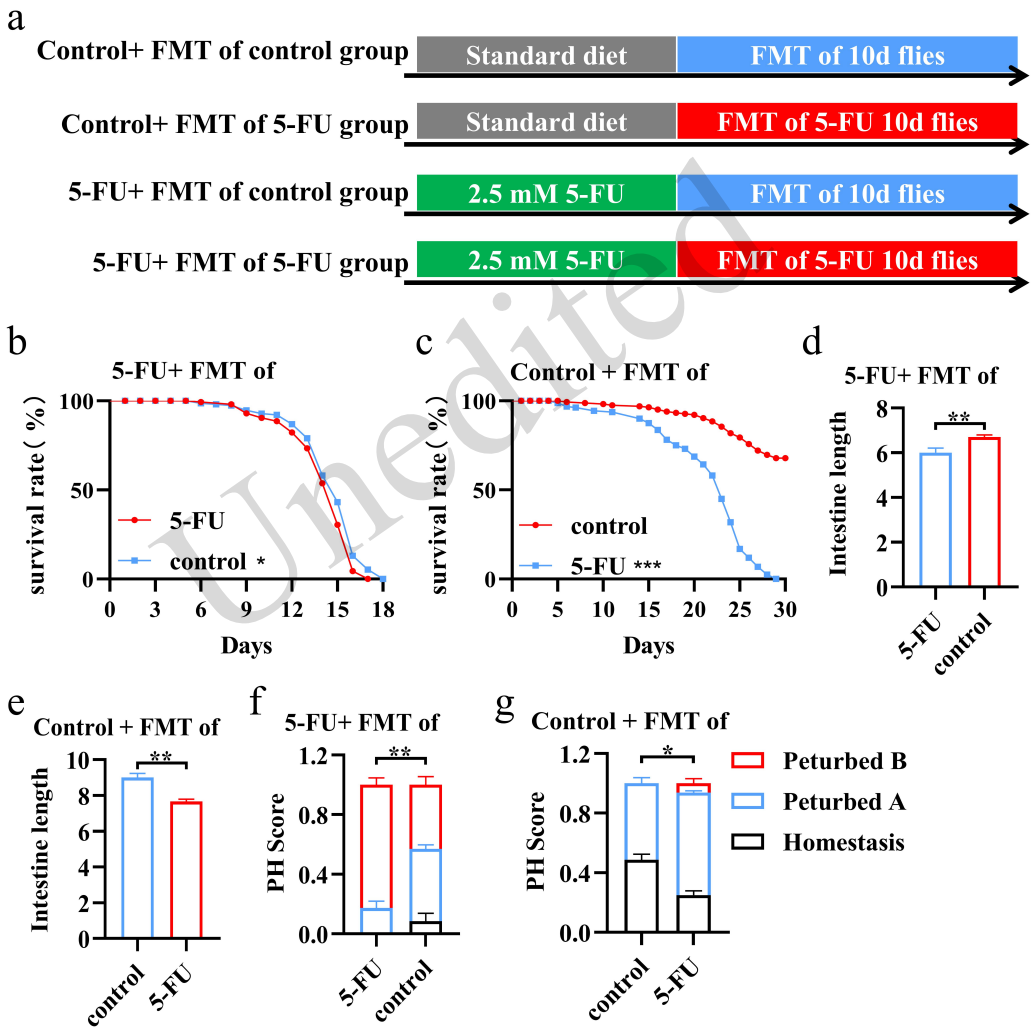

Fig.8 Gut microbiota dysbiosis contributes to 5-FU-induced intestinal damage in flies.

(a) Schematic timeline for the model establishment of FMT. (b-c) Survival rate (n=153–158). (d-e) Intestinal length (n=16). (f-g) PH score (n=3). Values are presented as mean±SEM. FMT, fecal microbiota transplantation. Data are presented as mean ± SEM, two-sided unpaired t-tests with Welch's correction; *$p < 0.05$, **$p < 0.01$, ***$p < 0.001$.

3.9 Exposure to 5-FU induces intestinal injury and ferroptosis in mice

To certify the damaging effects of 5-FU on the mouse intestine, mice were intraperitoneally injected with 5-FU for 4 days (Fig. 9a). Compared to the control, 5-FU supplementation decreased body weight, and shortened the intestinal length (Figs. 9b-9d). Also, 5-FU treatment also decreased the length of villi and crypts, increased the “villi length/crypt length” ratio, and induced inflammatory cell infiltration, villous edema, and

vasodilation (Figs. 9e-9h), indicating that 5-FU treatment could induce serious intestinal injury. Furthermore, to investigate whether ferroptosis is a conserved mechanism in 5-FU-induced intestinal injury, we measured the protein levels of glutathione peroxidase 4 (GPX4), 4-hydroxynonenal (4-HNE), long-chain acyl-CoA synthetase 4 (ASCL4), and Nrf2. The results showed that supplementation with 5-FU resulted in a decreased GPX4 protein level (Figs. 9e and 9i), which serves as the principal oxidoreductase utilizing glutathione as the primary reducing cofactor to neutralize lipid peroxidation byproducts (Xie et al., 2023). Administration of 5-FU increased the reactive lipid mediator level of 4-HNE (Figs. 9e and 9j) and the protein level of ASCL4 (Figs. 9e and 9k), which has a marked preference for activating PUFAs (Lin et al., 2024). In addition, 5-Fu treatment decreased the Nrf2 protein level and increased the ROS level (Figs. 9l-9o). Together, these results certified that ferroptosis was a pivotally conserved mechanism of 5-FU-induced IM in mice. Overall, this study established an in vivo model of 5-FU-induced IM in flies, uncovered a crucial role of gut microbiota-mediated ferroptosis and immune response in 5-FU-induced IM.

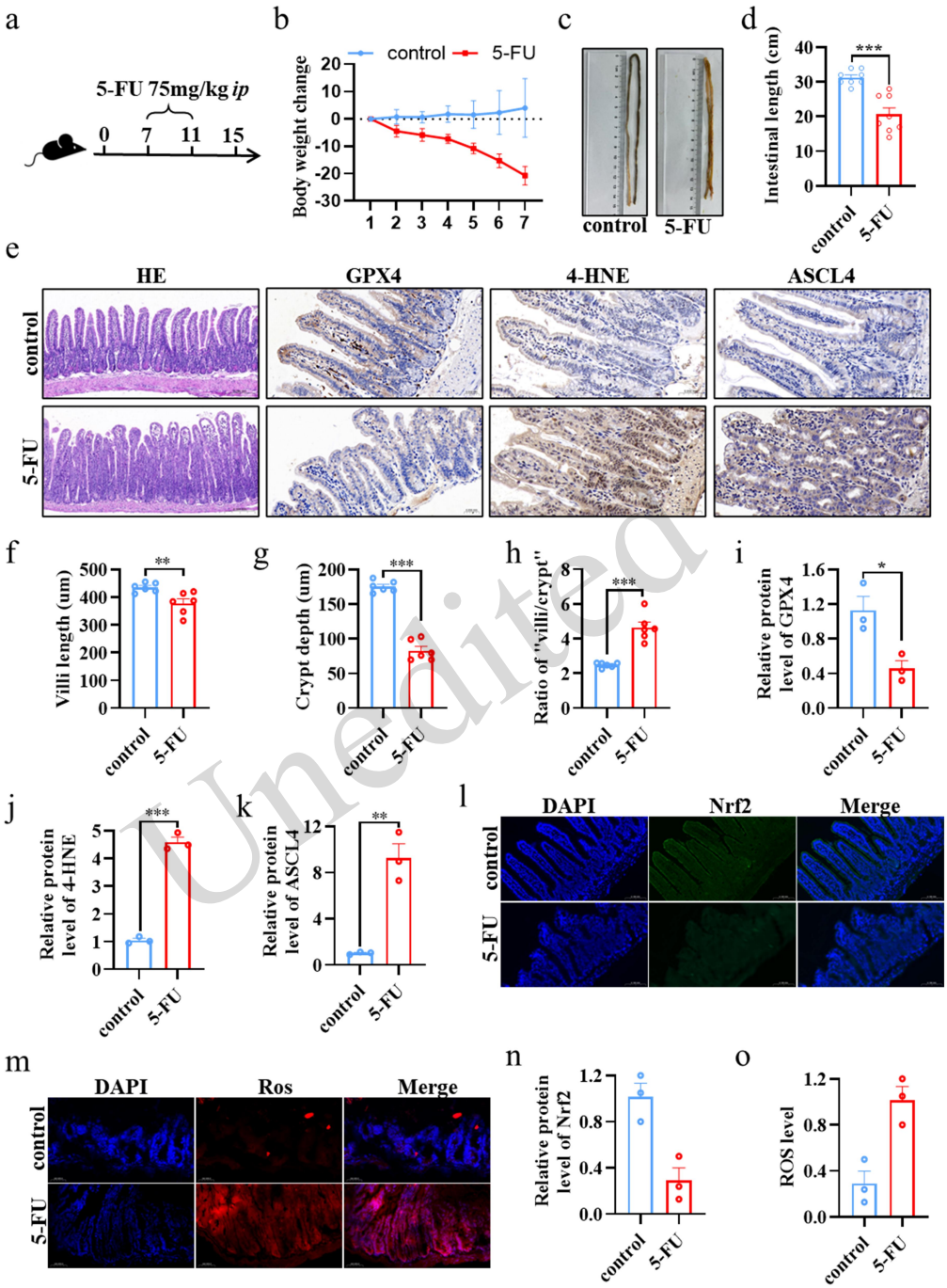

Fig.9. Exposure to 5-FU induces intestinal injury and ferroptosis in mice.

(a) Schematic timeline for the model establishment of 5-FU-induced IM. (b) Body weight (n=8). (c-d) The length of small intestines (n=8). (e) Representative microphotograph showing the histologic section of a longitudinally cut intestinal segment of control and 5-FU groups. GPX4, 4-HNE, and ASCL4 immunostaining of the jejunum of control and 5-FU groups. (f) Villi length (um) (n=6). (g) Crypt depth (um) (n=6). (h) Ratio of "villi length/crypt depth" (n=6). (i) The relative protein level of GPX4 (n=3). (j) The relative protein level of 4-HNE (n=3). (k) The relative protein level of ASCL4 (n=3). (l) Immunofluorescence of Nrf2. (m) Immunofluorescence of ROS. (n) The relative protein level of Nrf2 (n=3). (o) The ROS level (n=3). 5-FU, 5-fluorouracil; IM, intestinal mucositis; GPX4, glutathione peroxidase 4; 4-HNE, 4-Hydroxynonenal; ASCL4, long-chain acyl-CoA synthetase 4; Nrf2: Nuclear factor erythroid 2-related factor 2; ROS: reactive oxygen species. Data are presented as mean ± SEM, two-sided unpaired t-tests with Welch's correction; *$p < 0.05$, **$p < 0.01$, ***$p < 0.001$.

4. Discussion

In the present study, we established a model of 5-FU induced-IM in *Drosophila melanogaster*, and uncovered the essential roles of gut microbiota, ferroptosis, and innate immune in 5-FU-induced IM. The results showed that exposure to 5-FU significantly induced systemic and intestinal damage, decreased the survival rate, anti-starvation ability, and the numbers of eggs laid, delaying larval development, increasing food intake and Smurf numbers, decreasing excretion and crop motility, shortening intestine length, and inducing acid-base homeostasis imbalance, enterocyte death, and reduced ISCs' capacity. Additionally, 5-FU exposure induced the dysbiosis of gut microbiota, which enhanced ferroptosis and the innate immune response, thereby inducing intestinal damage.

Chemotherapy can induce long-term and systemic toxicities, affecting a majority of cancer survivors, significantly interfering with their quality of life (Di Nardo, et al., 2022). The survival rate in a starvation environment reflects resistance to stress and detoxification (Rommelaere et al., 2024). We found that 5-FU exposure decreased the survival rate of adult flies under normal and starvation condition, indicating an overall damage. Ovarian toxicity is one of the most notable and prevalent side effects of chemotherapy in female cancer patients (Cosgrove and Salani, 2019). Our results showed that 5-FU exposure induced a significant fertility toxicity in female flies. Although prior research has demonstrated that chemotherapy compromises ovarian function by inducing excessive ROS-mediated ferroptosis (Zhang et al., 2023b), the precise mechanisms underlying chemotherapy-induced ovarian dysfunction remain unclear. In addition, we found that 5-FU induced developmental toxicity, especially damaging the crawl ability of larvae. Consistent with our research findings, administration of a single dose of 5-FU to pregnant rats on the 12th gestational day can induce malformations in the development of the fetal nervous system (Kumar et al., 2006). Overall, we demonstrated that it is possible to evaluate the overall toxicology of 5-FU in adult flies.

IM represents one of the most debilitating adverse effects of chemotherapy (Di Nardo, et al., 2022). In a previous randomized clinical trial, all patients who had received treatment with either 5-FU or gemcitabine were symptomatic, presenting with pain, weight loss, and/or dyspepsia (Cascinu et al., 1999). Due to its anatomical division into a crop that rhythmically constricts to pump ingested material into the midgut for enzymatic processing—similar to the mammalian stomach—and a strongly acidic copper cell region (CCR, pH<3), the quantitative assessment of the Drosophila melanogaster crop and CCR provides a functional model for gastric evaluation (Strand and Micchelli, 2011; Cai et al., 2020). We found that 5-FU supplementation decreased crop motility, and induced an imbalance in acid-base homeostasis of CCR, indicating a functional disturbance of the gastrointestinal tract. ISCs drive the regenerative processes critical for maintaining the function of the gastrointestinal epithelium and ensuring the health and survival of multicellular organisms (Jasper, 2020). We found that exposure to 5-FU induced the death of intestinal cells, decreased the proliferation of ISCs, and damage of IECs. Given the high similarity in intestinal function and structure between flies and humans (Lemaitre and Miguel-Aliaga, 2013), the reduced survival rate, diminished metabolic capacity, and gastrointestinal dysfunction induced by 5-FU feeding effectively model the manifestations of chemotherapy-induced IM in humans (such as weight loss, maldigestion, diarrhea, and reduced intestinal mucosal repair capacity). This indicates that *Drosophila melanogaster* can be a suitable in vivo model for studying chemotherapy-induced IM.

The pathophysiologic mechanisms of 5-FU-induced IM are complicated. In this study, transcriptomics combined with bioinformatics analysis revealed that 5-FU-induced IM involved multiple pathways, including ferroptosis and immune response. Existing research indicates that alterations in gut microbiota homeostasis promote the development of IM (Huang, et al., 2022); and therefore we also performed microbiome sequencing. We found that 5-FU increased the abundance of *Enterobacteriaceae* and *Acetobacteraceae*, and reduced the relative abundance of *Orbaceae* and *Lactobacillaceae* in flies. *Acetobacter persici* can accelerate aging processes and reduce longevity in flies (Onuma et al., 2023). Furthermore, 5-FU administration reduced

the relative abundance of spices *Lactobacillus species*, and increased the relative abundance of *Acetobacter_pasteurianus*, and decreased the relative abundance of *Lactobacillus_plantarum*. The administration of *Lactobacillus plantarum L168* ameliorated intestinal inflammation and colorectal cancer growth (Zhang et al., 2023a). An increased prevalence of *Proteobacteria* was also regarded as a potential diagnostic signature of dysbiosis and risk of disease (Shin et al., 2015). Notably, Spearman's correlation analysis showed that the intestinal injury, innate immunity, and ferroptosis are closely correlated with these significantly different bacteria. Thus, we proposed that the disturbance of gut microbiota may increase ferroptosis and innate immune response in intestinal tissue, which jointly contribute to 5-FU-induced IM.

Ferroptosis represents an autonomous, non-catalyzed chemical process driven by dysregulated iron metabolism and an imbalance of oxidative stress, which plays a pivotal role in mediating cellular demise (Stockwell, 2022). First, we explored whether ferroptosis was a key mechanism in 5-FU-induced IM. Our findings suggested that 5-FU treatment elevated intestinal ROS levels and lipid peroxidation, while simultaneously increasing the expression of ferroptosis-related genes in flies. The potent ferroptosis inhibitor Fer-1 acts primarily by eliminating initiating lipid hydroperoxides in the presence of ferrous iron (Miotto et al., 2020). Intake of Fer-1 significantly increased the survival rate and intestinal length of 5-FU-treated flies in this study. Based on the above validation, ferroptosis can be considered a key mechanism in 5-FU-induced IM.

The activation of the innate immune response is a direct response to a disordered gut microbiota in flies (Leclerc and Reichhart, 2004; Iatsenko, et al., 2016; Chen, et al., 2022). The IMD-NF- κ B signaling pathway is activated in response to Gram-negative bacterial DAP-type peptidoglycans, which initiates the IMD cascade and subsequent activation of the Relish (*Rel*) transcription factor (Iatsenko, et al., 2016). In contrast, the Toll-NF-kB signaling is activated by Gram-positive bacterial Lysine-type peptidoglycans and fungal β-(1,3)-glucan via binding to PGRP-SA and glucan-binding proteins, respectively, to cleave cytokine Spaetzle and activate Toll receptor as well as the Dorsal-Dif transcriptional complex (Wang et al., 2006). Abs are commonly used to eliminate microorganisms in *Drosophila melanogaster*, serving as a method for generating gnotobiotic flies (Chen, et al., 2022). Here, Abs treatment significantly alleviated intestinal damage and activated the immune response induced by 5-FU. Meanwhile, FMT from 5-FU-treated flies injected into healthy flies caused intestinal damage in the recipient flies, whereas FMT from healthy flies injected into 5-FU-treated flies mitigated intestinal damage in the latter. These findings demonstrated that gut microbiota dysbiosis exacerbated 5-FU-induced IM in flies, which may be mediated by an activated immune response.

Previous studies have demonstrated that the gut microbiota modulates ferroptosis via its microbial constituents, functional activities, and metabolic products in several gastrointestinal disorders (Deng et al., 2021a), including intestinal I/R injury (Wang, et al., 2024a), and colorectal cancer (Cui et al., 2024). Thus, it is highly likely that gut microbiota-mediated ferroptosis is also a key mechanism in 5-FU-induced IM, yet the relationship between the two in this intestinal disorder remains unexplored. This study found that after antibiotic feeding eliminated the gut microbiota, the indicators of intestinal ferroptosis decreased in 5-FU-treated flies, indicating that gut microbiota-mediated ferroptosis was involved in the development of 5-FU-induced IM. However, this study did not investigate how chemotherapy-induced disruption of the microbiota regulates ferroptosis, which subsequently leads to intestinal injury. Future research should consider whether chemotherapy regulates ferroptosis by inducing specific bacteria or microbial metabolites, and through which signaling pathways the gut microbiota mediates the occurrence of ferroptosis.

The mouse is the most commonly used model organism for studying chemotherapy- IM (Mohammed, et al., 2023a). To validate the similarity between the *Drosophila melanogaster* IM model established in this study and mammalian systems, we utilized a 5-FU-induced mouse IM model to analyze indicators related to ferroptosis. The results showed that 5-FU treatment led to weight loss and intestinal shortening in mice, along with the activation of an evolutionarily conserved ferroptosis pathway, as evidenced by increased levels of ROS, ACSL4, and 4-HNE, and decreased GPX4 expression. Thus, the files can serve as a convenient and efficient model for studying 5-FU-induced IM. However, although *Drosophila melanogaster* and mice share

conservation in intestinal function, tissue structure, and core signaling pathways(Lemaitre and Miguel-Aliaga, 2013), certain species-specific differences remain. The gut microbiota of *Drosophila melanogaster* is relatively simple (Lemaitre and Miguel-Aliaga, 2013), which facilitates germ-free operations and colonization studies (Lemaitre and Miguel-Aliaga, 2013). Its immune system primarily relies on innate immunity, which is dependent on the IMD and Toll pathways, and lacks adaptive immune components (Lemaitre and Miguel-Aliaga, 2013). Therefore, while mechanistic studies in *Drosophila melanogaster* help reveal evolutionarily conserved core regulatory mechanisms (e.g., the functions of GPX4 and ACSL families), its relatively simple physiological structure creates some distance from the complexity of human disease

In conclusion, combining *Drosophila melanogaster* and mouse models holds significant potential for future screening of therapeutic strategies against chemotherapy-induced IM. This integrated approach leverages the strengths of both models: efficient preliminary screening in *Drosophila melanogaster* and in-depth mechanistic validation in mice, offering the dual advantages of efficiency and depth.

5. Conclusion

The present study establishes a 5-FU-induced IM in *Drosophila melanogaster*; elucidating the role of gut microbiota-dependent ferroptosis in 5-FU-induced IM. Regarding model construction, 5-FU exposure induced systemic damage, fertility and developmental toxicity, and enterocyte damage, while also decreasing the proliferation of ISCs. Mechanistically, 5-FU-induced disordered gut microbiota may induce IM by activating innate immunity and ferroptosis. Overall, these findings establish a precise and efficient IM model for potential future application in drug screening.

Data availability statement

The data and custom code that support the findings from this study are available from the corresponding author upon reasonable request.

Acknowledgments

This work is supported by the Joint Research Fund major projects (No. 24JRRA875), Foundation from Key Laboratory of Dunhuang Medicine (No. DHYX22-01), and Gansu Natural Science Foundation (No. 23JRRA1202 and 25JRRA1177).

Author contributions

Jianzheng HE and Yongqi LIU contributed to conceptualization, funding acquisition, and supervision. Xiaoqian WANG and Minghui XIU performed the experimental research and data analysis, wrote and edited the manuscript. Linghui CHANG and Yan WANG performed the establishment of animal models. Linghui CHANG and Jinhan WU contributed to the study design, data analysis, writing and editing of the manuscript. All authors read and approved the final manuscript and, therefore, had full access to all the data in the study and take responsibility for the integrity and security of the data.

Compliance with ethics guidelines

Jianzheng HE, Yongqi LIU, Xiaoqian WANG, Minghui XIU, Linghui CHANG, Yan WANG, and Jinhan WU declare that they have no conflict of interest.

The mouse protocols were approved by the Institutional Animal Care and Use Committee of Gansu University of Chinese Medicine (approval number: SY2024-264), conducted in compliance with their guidelines and the GB/T 35892-2018 Guidelines for Ethical Review of Laboratory Animal Welfare.

References

Bettedi L, Aslam MF, Szular J, et al., 2011. Iron depletion in the intestines of malvolio mutant flies does not occur in the absence of a multicopper oxidase. *J Exp Biol*, 214(Pt 6):971-978. https://doi.org/10.1242/jeb.051664

Bilak A, Su TT, 2009. Regulation of drosophila melanogaster pro-apoptotic gene hid. Apoptosis, 14(8):943-949. https://doi.org/10.1007/s10495-009-0374-2

Cai J, Xi J, Wei Y, 2020. Measuring crop motility and food passaging in drosophila. *J Vis Exp*, (159) https://doi.org/10.3791/61181

Cascinu S, Silva RR, Barni S, et al., 1999. A combination of gemcitabine and 5-fluorouracil in advanced pancreatic cancer, a report from the italian group for the study of digestive tract cancer (giscad). *Br J Cancer*, 80(10):1595-1598. https://doi.org/10.1038/sj.bjc.6690568

Chen Y, Xu W, Chen Y, et al., 2022. Renal nf-kappab activation impairs uric acid homeostasis to promote tumor-associated mortality independent of wasting. *Immunity*, 55(9):1594-1608 e1596. https://doi.org/10.1016/j.immuni.2022.07.022

Cosgrove CM, Salani R, 2019. Ovarian effects of radiation and cytotoxic chemotherapy damage. *Best Pract Res Clin Obstet Gynaecol*, 55:37-48. https://doi.org/10.1016/j.bpobgyn.2018.07.008

Cui W, Guo M, Liu D, et al., 2024. Gut microbial metabolite facilitates colorectal cancer development via ferroptosis inhibition. *Nat Cell Biol*, 26(1):124-137. https://doi.org/10.1038/s41556-023-01314-6

Deng F, Zhao BC, Yang X, et al., 2021a. The gut microbiota metabolite capsiate promotes gpx4 expression by activating trpv1 to inhibit intestinal ischemia reperfusion-induced ferroptosis. *Gut Microbes*, 13(1):1-21. https://doi.org/10.1080/19490976.2021.1902719

Deng S, Wu D, Li L, et al., 2021b. Tbhq attenuates ferroptosis against 5-fluorouracil-induced intestinal epithelial cell injury and intestinal mucositis via activation of nrf2. *Cell Mol Biol Lett*, 26(1):48. https://doi.org/10.1186/s11658-021-00294-5

Di Nardo P, Lisanti C, Garutti M, et al., 2022. Chemotherapy in patients with early breast cancer: Clinical overview and management of long-term side effects. *Expert Opin Drug Saf*, 21(11):1341-1355. https://doi.org/10.1080/14740338.2022.2151584

Elad S, Cheng KKF, Lalla RV, et al., 2020. Mascc/isoo clinical practice guidelines for the management of mucositis secondary to cancer therapy. *Cancer*, 126(19):4423-4431. https://doi.org/10.1002/cncr.33100

Ge X, Fan YZ, Deng Y, et al., 2025. Pectolinarigenin mitigates 5-fu-induced intestinal mucositis via suppressing ferroptosis through activating ppargamma/gpx4 signaling. *Phytomedicine*, 143:156843. https://doi.org/10.1016/j.phymed.2025.156843

He J, Li X, Yang S, et al., 2022b. Protective effect of astragalus membranaceus and its bioactive compounds against the intestinal inflammation in drosophila. *Front Pharmacol*, 13:1019594. https://doi.org/10.3389/fphar.2022.1019594

Horowitz J, Chargaff E, 1959. Massive incorporation of 5-fluorouracil into a bacterial ribonucleic acid. *Nature*, 184:1213-1215. https://doi.org/10.1038/1841213a0

Huang B, Gui M, Ni Z, et al., 2022. Chemotherapeutic drugs induce different gut microbiota disorder pattern and nod/rip2/nf-kappab signaling pathway activation that lead to different degrees of intestinal injury. *Microbiol Spectr*, 10(6):e0167722. https://doi.org/10.1128/spectrum.01677-22

Iatsenko I, Kondo S, Mengin-Lecreulx D, et al., 2016. Pgrp-sd, an extracellular pattern-recognition receptor,

enhances peptidoglycan-mediated activation of the drosophila imd pathway. *Immunity*, 45(5):1013-1023.
https://doi.org/10.1016/j.immuni.2016.10.029

Jasper H, 2020. Intestinal stem cell aging: Origins and interventions. *Annu Rev Physiol*, 82:203-226. https://doi.org/10.1146/annurev-physiol-021119-034359

Jurica J, Turjap M, 2025. Management of gastrointestinal side effects of cancer pharmacotherapy: Part 1: Diarrhoea, constipation, mucositis and anorexia. *Ceska Slov Farm*, 73(4):222-227. https://doi.org/10.36290/csf.2024.040

Kong P, Yang M, Wang Y, et al., 2023. Ferroptosis triggered by stat1- irf1-acsl4 pathway was involved in radiation-induced intestinal injury. *Redox Biol*, 66:102857. https://doi.org/10.1016/j.redox.2023.102857

Kumar S, Lobo SW, Dubey AK, et al., 2006. Teratogenic effects of 5-fluorouracil on rat brain. *Nepal Med Coll J*, 8(1):7-8.
https://pubmed.ncbi.nlm.nih.gov/16827081/

Leclerc V, Reichhart JM, 2004. The immune response of drosophila melanogaster. *Immunol Rev*, 198:59-71. https://doi.org/10.1111/j.0105-2896.2004.0130.x

Lemaitre B, Miguel-Aliaga I, 2013. The digestive tract of drosophila melanogaster. *Annu Rev Genet*, 47:377-404.
https://doi.org/10.1146/annurev-genet-111212-133343

Lenfers BH, Loeffler TM, Droege CM, et al., 1999. Substantial activity of budesonide in patients with irinotecan (cpt-11) and 5-fluorouracil induced diarrhea and failure of loperamide treatment. *Ann Oncol*, 10(10):1251-1253.
https://doi.org/10.1023/a:1008390308416

Li X, Yang S, Wang S, et al., 2023. Regulation and mechanism of astragalus polysaccharide on ameliorating aging in drosophila melanogaster. *International Journal of Biological Macromolecules*, 234 (2023): 123632.
https://doi.org/10.1016/j.ijbiomac.2023.123632

Li Y, Feng D, Wang Z, et al., 2019. Ischemia-induced acsl4 activation contributes to ferroptosis-mediated tissue injury in intestinal ischemia/reperfusion. *Cell Death Differ*, 26(11):2284-2299. https://doi.org/10.1038/s41418-019-0299-4

Lin Z, Long F, Kang R, et al., 2024. The lipid basis of cell death and autophagy. *Autophagy*, 20(3):469-488. https://doi.org/10.1080/15548627.2023.2259732

Liu W, Zhou X, Xiao L, et al., 2025. The gut microbiota-mediated ferroptosis pathway: A key mechanism of ginsenoside rd against metabolism-associated fatty liver disease. *Chin Med*, 20(1):83. https://doi.org/10.1186/s13020-025-01121-1

Mandilaras K, Pathmanathan T, Missirlis F, 2013. Iron absorption in drosophila melanogaster. *Nutrients*, 5(5):1622-1647.
https://doi.org/10.3390/nu5051622

Miotto G, Rossetto M, Di Paolo ML, et al., 2020. Insight into the mechanism of ferroptosis inhibition by ferrostatin-1. *Redox Biol*, 28:101328.
https://doi.org/10.1016/j.redox.2019.101328

Mohammed AI, Celentano A, Paolini R, et al., 2023a. Characterization of a novel dual murine model of chemotherapy-induced oral and intestinal mucositis. *Sci Rep*, 13(1):1396. https://doi.org/10.1038/s41598-023-28486-3

Mohammed AI, Celentano A, Paolini R, et al., 2023b. High molecular weight hyaluronic acid drastically reduces chemotherapy-induced mucositis and apoptotic cell death. *Cell Death Dis*, 14(7):453. https://doi.org/10.1038/s41419-023-05934-6

Onuma T, Yamauchi T, Kosakamoto H, et al., 2023. Recognition of commensal bacterial peptidoglycans

defines drosophila gut homeostasis and lifespan. *PLoS Genet*, 19(4):e1010709. https://doi.org/10.1371/journal.pgen.1010709

Orgad S, Nelson H, Segal D, et al., 1998. Metal ions suppress the abnormal taste behavior of the drosophila mutant malvolio. *J Exp Biol*, 201(Pt 1):115-120. https://doi.org/10.1242/jeb.201.1.115

Peterson LW, Artis D, 2014. Intestinal epithelial cells: Regulators of barrier function and immune homeostasis. *Nat Rev Immunol*, 14(3):141-153. https://doi.org/10.1038/nri3608

Reiff T, Jacobson J, Cognigni P, et al., 2015. Endocrine remodelling of the adult intestine sustains reproduction in drosophila. *e*Life, 4:e06930. https://doi.org/10.7554/eLife.06930

Rommelaere S, Carboni A, Bada Juarez JF, et al., 2024. A humoral stress response protects drosophila tissues from antimicrobial peptides. *Curr Biol*, 34(7):1426-1437 e1426. https://doi.org/10.1016/j.cub.2024.02.049

Ru Q, Li Y, Chen L, et al., 2024. Iron homeostasis and ferroptosis in human diseases: Mechanisms and therapeutic prospects. *Signal Transduct Target Ther*, 9(1):271. https://doi.org/10.1038/s41392-024-01969-z

Shi N, Li N, Duan X, et al., 2017. Interaction between the gut microbiome and mucosal immune system. *Mil Med Res*, 4:14. https://doi.org/10.1186/s40779-017-0122-9

Shin NR, Whon TW, Bae JW, 2015. Proteobacteria: Microbial signature of dysbiosis in gut microbiota. *Trends Biotechnol*, 33(9):496-503. https://doi.org/10.1016/j.tibtech.2015.06.011

Stockwell BR, 2022. Ferroptosis turns 10: Emerging mechanisms, physiological functions, and therapeutic applications. *Cell*, 185(14):2401-2421. https://doi.org/10.1016/j.cell.2022.06.003

Strand M, Micchelli CA, 2011. Quiescent gastric stem cells maintain the adult drosophila stomach. *Proc Natl Acad Sci U S A*, 108(43):17696-17701. https://doi.org/10.1073/pnas.1109794108

Teschke R, 2024. Hemochromatosis: Ferroptosis, ros, gut microbiome, and clinical challenges with alcohol as confounding variable. *Int J Mol Sci*, 25(5):2668. https://doi.org/10.3390/ijms25052668

Wang F, Liu X, Huang F, et al., 2024a. Gut microbiota-derived gamma-aminobutyric acid from metformin treatment reduces hepatic ischemia/reperfusion injury through inhibiting ferroptosis. *Elife*, 12:12:RP89045. https://doi.org/10.7554/eLife.89045

Wang L, Weber AN, Atilano ML, et al., 2006. Sensing of gram-positive bacteria in drosophila: Gnbp1 is needed to process and present peptidoglycan to pgrp-sa. *EMBO J*, 25(20):5005-5014. https://doi.org/10.1038/sj.emboj.7601363

Wang Y, Qin Y, Kang Q, et al., 2024b. Therapeutic potential of astragalus membranaceus-pueraria lobata decoction for the treatment of chemotherapy bowel injury. *FASEB J*, 38(19):e70102. https://doi.org/10.1096/fj.202401677R

Wei JJ, Li XJ, Liu W, et al., 2023. Eucommia polysaccharides ameliorate aging-associated gut dysbiosis: A potential mechanism for life extension in drosophila. *Int J Mol Sci*, 24(6):5881. https://doi.org/10.3390/ijms24065881

Wei Y, Xi J, Cai J, 2020. Measuring crop motility and food passaging in drosophila. *Journal of Visualized Experiments*, (159):10.3791/61181. https://doi.org/10.3791/61181-v

Xia Y, Wang H, Xie Z, et al., 2024a. Inhibition of ferroptosis underlies egcg mediated protection against parkinson's disease in a drosophila model. *Free Radical Biology and Medicine*, 211:63-76. https://doi.org/10.1016/j.freeradbiomed.2023.12.005

Xia Y, Wang H, Xie Z, et al., 2024b. Inhibition of ferroptosis underlies egcg mediated protection against parkinson's disease in a drosophila model. *Free Radic Biol Med*, 211:63-76. https://doi.org/10.1016/j.freeradbiomed.2023.12.005

Xie Y, Kang R, Klionsky DJ, et al., 2023. Gpx4 in cell death, autophagy, and disease. *Autophagy*, 19(10):2621-2638. https://doi.org/10.1080/15548627.2023.2218764

Xiu M, Li B, He L, et al., 2025. Caffeic acid protects against ulcerative colitis via inhibiting mitochondrial apoptosis and immune overactivation in drosophila. *Drug Des Devel Ther*, 19:2157-2172. https://doi.org/10.2147/DDDT.S499284

Zhang Q, Zhao Q, Li T, et al., 2023a. Lactobacillus plantarum-derived indole-3-lactic acid ameliorates colorectal tumorigenesis via epigenetic regulation of cd8(+) t cell immunity. *Cell Metab*, 35(6):943-960 e949. https://doi.org/10.1016/j.cmet.2023.04.015

Zhang S, Liu Q, Chang M, et al., 2023b. Chemotherapy impairs ovarian function through excessive ros-induced ferroptosis. *Cell Death Dis*, 14(5):340. https://doi.org/10.1038/s41419-023-05859-0